THE BALTIC JOURNAL
OF ROAD AND BRIDGE ENGINEERING
2025/20(1)

SSN 1822-427X/eISSN 1822-4288
2025 Volume 20 Issue 1: 1–44
https://doi.org/10.7250/bjrbe.2025-20.652

OPTIMIZING SBS & TIRE PYRO OIL MODIFIED VG 30 BITUMEN FOR SUSTAINABLE PAVEMENTS

SAURABH KULKARNI[1*], HEMANT HADOLE[2], NIKITA BHAGAT[2], MAHADEO RANDIVE[2]

[1]*Dept. of Civil Engineering, MES Wadia College of Engineering, Pune, 411001, India*
[2]*Dept. of Civil Engineering, College of Engineering, Pune, 411005, India*

Received 12 March 2024; accepted 7 February 2025

Abstract. In recent years, Indian roads have experienced a significant increase in axle load and traffic volume, necessitating improved performance in top bituminous layers. While Indian guidelines recommend VG 40 grade bitumen for perpetual pavements, its limited supply prompts widespread use of VG 30 grade bitumen. This study explores the viability of modified VG 30 bitumen, employing Styrene Butadiene Styrene (SBS) and Tire pyro oil (TPO) as modifiers, as an alternative to VG 40. Rheological tests, including Dynamic Shear Rheometer and Brookfield Viscometer, alongside morphological and chemical analyses, ascertain the optimal SBS dosage. Addition of TPO, ranging from 1% to 3%, reduces mixing and compaction temperatures. Marshall Stability and Indirect Tensile Strength tests compare strength characteristics. Sixteen perpetual pavement sections are designed based on Indian guidelines, comparing thickness, life cycle cost, and carbon dioxide emissions over five decades. Modified VG 30 binder exhibits only a slight increase in thickness compared to unmodified VG 40 binder, while significantly reducing life cycle costs and carbon dioxide emissions. Experimental results suggest that modified VG 30 with 3% SBS, and optionally with 1% TPO, can effectively replace VG 40 grade bitumen for perpetual pavements to address its supply issue.

* Corresponding author. E-mail: saurabh.kulkarni@mescoepune.org

Saurabh KULKARNI (ORCID ID 0000-0003-1908-0947)
Hemant HADOLE (ORCID ID 0000-0002-4907-1454)
Nikita BHAGAT (ORCID ID 0000-0002-4297-9718)
Mahadeo RANDIVE (ORCID ID 0000-0002-6919-1189)

Keywords: bitumen modification, pavement design, perpetual pavement, sustainable pavements.

Introduction

Due to difference in climatic condition in various places, careful selection of bitumen is very important for longevity of pavement. Due to exponential growth of traffic volumes in a country like India, limitations in use of conventional bitumen are clearly visible. Continuous maintenance work due to premature failure of roads is a regular occurrence. The performance of bituminous mix is closely related to the properties of bitumen used in it. For distress control in pavement, bitumen mix should have enhanced properties to resist rutting, cracking, fatigue, stripping etc. For improvement in bitumen properties, polymer modification is generally proposed (IRC 37, 2018). The modification can help improve service period of pavement. Among various available polymers, elastomers are widely used in bitumen modification (Ranadive et al., 2018). Among the elastomeric polymers, SBS is used in the present study. It consists of two monomers, Styrene and Butadiene. SBS polymer helps increase hardness of bitumen due to presence of styrene and it also helps improve thermal cracking resistance due to presence of butadiene (Emery & O'connell, 1999). Various studies have observed that SBS modification improves the performance of bituminous mixes (Airey, 2003; Tayfur et al., 2007). Modified binder using SBS copolymers with 30% styrene by weight exhibited the best conventional properties (Zhang et al., 2014). One disadvantage of SBS modification results in higher mixing and compaction temperature (Tayfur et al., 2007). In case of higher temperatures, viscosity of binder plays an important role for permeability. Polymer modification does have an effect on viscosity of the bituminous mixture. As the SBS percentage increases, viscosity of binder increases and more of its quantity is required in coating the same quantity of aggregate. Though SBS modified binder provides sufficient resilient modulus for use in construction of pavement, it is necessary to decrease mixing and compaction temperature. In pursue of this objective, this study investigates the use of TPO in modified binder without much adverse effect on required properties of binder.

Over one billion tires are manufactured worldwide and a similar number of tires are permanently removed from vehicles resulting in wastage. India contributes around 6% to 7% of worldwide total. India's tire industry grows at 12% per year and, thus, scrapped tire numbers are also increasing. It is estimated that waste tire generation increases at a rate of 4% per year (Yu, 2008). Modern rubber tires are reinforced with elements like metal and chemical additives. Tires must have anti-aging, wear resistance, and failure resistance properties in order to function properly. Waste tires are highly resistant to physical, chemical, and biological

degradation, which makes it difficult for such tires to self-degrade. This complex nature of modern tires makes them difficult to treat when they are scrapped. The methods like landfilling and stockpiling are adopted in dealing with tire waste. These methods expose the communities to health risk and contribute to environmental pollution. Pyrolysis of scrapped tires is one way to deal with the disposal issue. Pyrolysis process transforms waste into oil, char and gas. The oil is separated and can be used as liquid fuel (Roy et al., 1999; Murugan et al., 2009). Char and oil can be used to improve high temperature and low temperature properties of bitumen, respectively (Chaala et al., 1999; Yousefi, 2004). The pyrolysis of waste tires is typically carried out in anoxic or inert gas environments under high temperature and pressure. The products include about 40% pyrolysis oil, 35% solid carbon black, 12% steel wire, and 13% combustible gas (Lehmann et al., 1998). There is a lot of interest in dealing with waste tires in an economically sound way, and this process is considered one of the best options. The pyrolysis of waste tires can produce a high-quality product that can be reused or recycled. It is an environmentally friendly way to deal with waste tires.

In recent years, there has been a surge in exploring various technologies to enhance the properties of bitumen. Among these, researchers have increasingly turned to waste plastics as a means to bolster the performance of rubberized bitumen, particularly in mitigating plastic deformation. Notably, studies have underscored the potential of recycling plastic and rubber waste in augmenting the performance of bituminous concrete (Xu et al., 2021; Movilla-Quesada et al., 2019; Lastra-González et al.,2022). Lyu et al. (2021) highlighted the enhancement of self-healing properties in asphalt through the incorporation of Polyurethane elastomer, while Zhang et al. (2019) demonstrated the efficacy of crumb rubber derived from waste tires in improving bitumen performance and curbing environmental pollution. The incorporation of crumb rubber has shown significant promise in enhancing bitumen's resistance to rutting, low-temperature cracking, and fatigue, as evidenced by previous research findings. Consequently, waste plastics and crumb rubber emerge as effective additives for enhancing the technical properties of bitumen, offering a sustainable approach to reusing and recycling waste tires. Thus, the development of tire recycling technologies becomes imperative to ensure environmentally sound treatment. Notably, tire re-treading, incineration for energy generation, production of rubber powder, and pyrolysis represent common avenues for waste tire recycling (Formela, 2021). However, it is essential to note that waste tire incineration yields polycyclic aromatic hydrocarbons, posing carcinogenic risks (Mastral et al., 1999). Despite this characteristic, rubber powder exhibits commendable anti-fatigue, anti-rutting, and ice resistance properties when used as a bitumen modifier (Xiao et al., 2010; Niu et al., 2021). Nonetheless, the energy-intensive process of grinding and refining required for rubber powder preparation, coupled with the complexity of rubber bitumen formulation and the

need for specialized equipment, presents significant challenges (Ansari et al., 2021). Additionally, achieving optimal technical performance necessitates adequate wetting of rubber powder during the blending process, mandating sufficient swelling and development time (Tabatabaee & Kurth, 2017). These challenges have hindered the widespread adoption of rubber powder-modified bitumen. Moreover, research on alternative additives for bitumen modification, such as waste vegetable oil, engine oil, bio-oil, and soybean oil, suggests their potential in improving bitumen's low-temperature crack resistance and fatigue properties (Hugener et al., 2013; Fini et al., 2011; Lv et al., 2021). Chaala et al. (1999) explored the feasibility of enhancing bitumen using components of TPO obtained at high temperatures, revealing promising results. However, the combined effects of SBS and TPO composites in bitumen modification remain unclear, though they may potentially address each constituent's shortcomings, leading to improved modification effects.

In countries like India, where resources are scarce and infrastructure funding is limited, the longevity of pavements is crucial. The lifespan of flexible pavements hinges on various factors such as traffic volume, axle load properties, design methodologies, material selection, climatic conditions, and maintenance practices. To ensure durable pavements, rut-resistant mixtures are essential, particularly for perpetual pavements. Conventional bitumen mixes often lack the required resilient modulus for perpetual pavements. Therefore, achieving a high resilient modulus in bituminous mixes, particularly with readily available binders like VG 30 due to constraints in the supply of VG 40 binder, is imperative (Mittal et al., 2018). Hence, this study investigates the impact of SBS modification in VG 30 bitumen and the addition of TPO in SBS-modified mixes for their applicability in long-lasting pavements.

The current research assesses the rutting performance of modified and unmodified bituminous mixes using various rutting parameters to determine their suitability for rutting resistance evaluation. The optimum SBS content in VG 30 and the optimal TPO content in SBS-modified binder were determined through conventional, rheological, and morphological analyses. Additionally, the strength characteristics of SBS-modified bitumen with and without TPO were evaluated using Marshall Stability test (MST) and Indirect Tensile Strength (ITS) test. Furthermore, this study compares the properties of modified and unmodified VG 30 mixes with unmodified VG 40 grade concerning fundamental properties, rutting resistance, strength characteristics, and perpetual pavement design.

1. Materials

The following materials are used in this study.

1.1. Bitumen

In this study, Indian standard viscosity-graded VG 30 bitumen sourced from the Indian oil refinery in Pune was employed to formulate both modified and unmodified bituminous mixtures. Thorough examination of the crucial properties of the bitumen was conducted, and the findings pertaining to the unmodified bitumen are presented in Table 1.

1.2. Styrene butadiene styrene (SBS)

To create modified bitumen, Styrene Butadiene Styrene (SBS) pellets were utilised. The properties of the SBS used in the study are outlined in Table 2.

1.3. Aggregate

The aggregates utilised in this research were sourced from a local quarry. Details regarding the conventional properties of the aggregates and their gradation are provided in Table 3 and Table 4, respectively. The selection of aggregate gradation adhered to the grading II specifications for the bituminous concrete layer as per MoRTH (2013) guidelines. To facilitate effective comparison among mixtures, the same gradation was adopted.

Table 1. Freight wagon bogies tested at the Kouvola railway yard

Property	Test Method	VG 30	VG 40
Penetration value	IS 1203-1978	52	42
Softening point	IS 1205-1978	49	62°C
Absolute viscosity at 60 °C, poises	IS 1206(part-II)-1978	2404	1.02
Kinematic viscosity at 135 °C, cSt.	IS 1206(part-III)-1978	457	74
Specific gravity	IS 1202-1978	1.0	3436
Ductility value at 25 °C	IS 1208-1978	86	575
Elastic recovery	IRC: SP 53-2010	26	35
High Temperature PG Grade		PG 64-XX	PG70-XX

Table 2. Properties of SBS

Property	Value	Standard/Specification
Specific gravity	0.98	ASTM D792
Styrene/rubber ratio	30/70	-
Melt index	<1 g/10 min	ASTM D1238
Shore hardness, A	70	ASTM D2240
Elongation at break, %	878	ASTM D412
Tensile strength at break, MPa	31.9	ASTM D412

Table 3. Aggregate properties

Composition	SBS	Allowable values as per MoRTh 2013	Standard/ Specification
Specific gravity (fine aggregate)	2.76	-	ASTM C127
Specific gravity (coarse aggregate)	2.70	-	ASTM C128
Impact value, %	21.50	Maximum 24%	IS:2386 Part 4
Crushing value, %	19.30		ASTM C131
Abrasion value, %	28.4	Maximum 30%	
Water absorption, %	0.35	Maximum 2%	ASTM C127
Flakiness and Elongation Index, %	26	Maximum 35%	IS:2386 Part 1

Table 4. Gradation of aggregate

Sr. No	Sieve Size, mm	Unit	Composition / Blending					Specification as per MoRTH Table No.500-17 (% Passing)	
		%	35	15	48	2	100		
			Coarse and Fine aggregate in mm						
			12 mm	06 mm	Crushed Sand	Stone Dust	Actual Total	Min	Max
1	19.0	%	35.00	15.00	48.00	2.00	100	-	100
2	13.2	%	31.58	15.00	48.00	2.00	96.58	90	100
3	9.5	%	14.03	15.00	48.00	2.00	79.03	70	88
4	4.75	%	0.00	10.14	48.00	2.00	60.14	53	71
5	2.36	%	0.00	2.73	43.24	2.00	47.96	42	58
6	1.18	%	0.00	0.00	37.97	2.00	39.97	34	48
7	0.60	%	0.00	0.00	29.95	2.00	31.95	26	38
8	0.30	%	0.00	0.00	20.69	1.94	22.63	18	28
9	0.15	%	0.00	0.00	13.89	1.65	15.54	12	20
10	0.075	%	0.00	0.00	4.78	1.48	6.26	4	10

1.4. Tire pyrolysis oil [TPO]

The tire pyrolysis oil used in this study is a liquid produced from the pyrolysis process of scrape tire. The oil used in this study was obtained from Devansh industries, Gaikwadwadi village near Pune City. TPO was obtained by thermal decomposition of small scrap tire pieces in pyrolysis plant at high temperature of 750 °C (Lehman, 1998). The properties of TPO used in this study are shown in Table 5.

Table 5. Material properties of TPO

Details	**Value**	**Standard/Specification (178-187)**
Colour	Opaque and Dark Brown	-
Flash Point, by PMCC °C	< 40	IS 1448
Density at 15 °C, kg/m^3	913	IS:1448
Water Content, by weight mg/kg	1580.7	IS 2362
Pour Point, °C	< –42	IS 1448
Gross Calorific Value, cal/g	9990	IS 1448
Ash Content, by mass, %	0.337	ASTM D482-13
Kinematic Viscosity at 60 °C, cSt	2.59	ASTM D 445-17A
Net Calorific Value, cal/g	9004	IS 1448
Total Sulphur, %	0.794	ASTM D 4294
Inorganic Acidity, Mg KOH/g	Nil	IS 1448
Ramsbottom Carbon Residue of Petroleum Products (on whole sample), % by wt	0.37	ASTM D 524

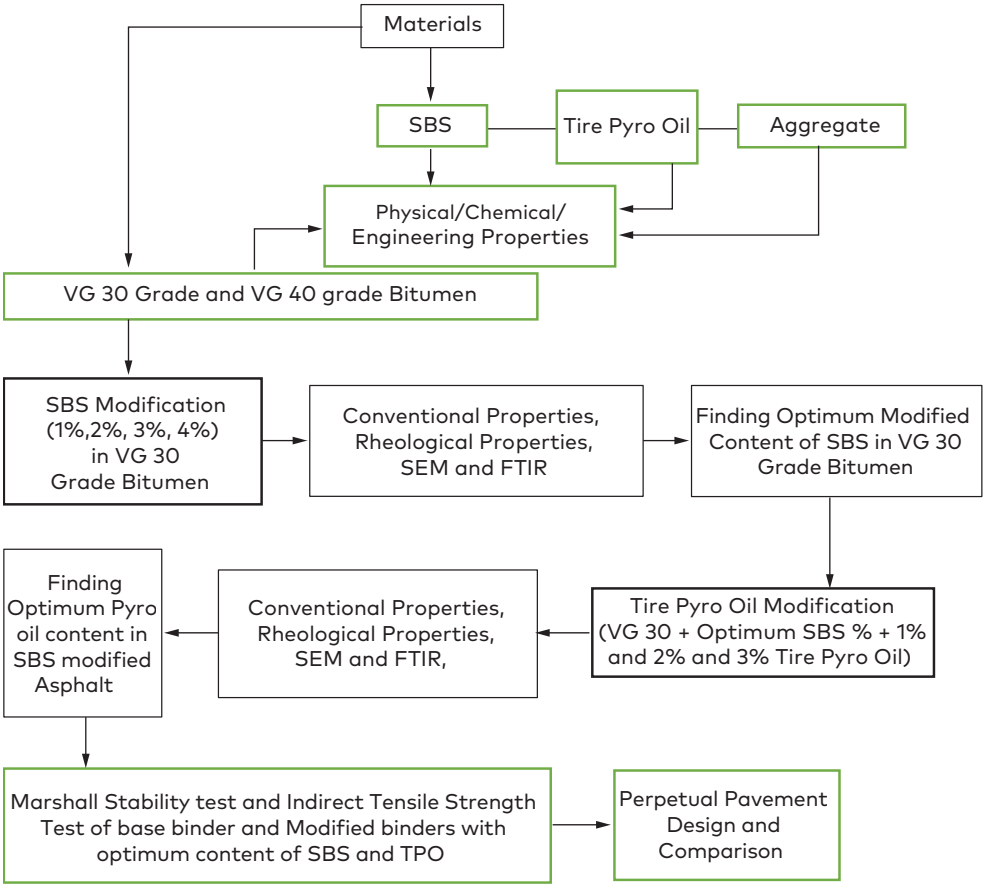

Figure 1. Details of the test program

2. Rutting parameter

Rutting occurs primarily due to inadequate structural strength of the bituminous binder and stands as a significant factor affecting the durability of flexible pavements. The Mechanistic-Empirical Pavement Design Guide (NCHRP, 2004) recommends considering a limiting value for the estimated mix rut depth, determined through mechanistic models, which should be lower than the acceptable rut depth throughout the pavement's service life. Historically, penetration and softening point tests were commonly employed to assess the rutting behaviour of bituminous binders. However, these conventional tests fail to accurately reflect the true rutting behaviour of bituminous binders (Sybilski, 1996). To address this

issue, various studies have been done (Anderson et al., 1994; Kennedy et al., 1994; Dongré et al., 2004; D'Angelo et al., 2007; Shenoy, 2008; Morea et al., 2011) and rutting parameters like complex shear modulus (G^*) and phase angle (δ), Superpave parameter, i.e., $G^*/\sin\delta$, damping coefficient (tanδ), Shenoy parameter, i.e., $G^*/[1-(1/\tan\delta\times\sin\delta)]$, Non-recoverable creep compliance (J_{nr}) have been proposed (Shenoy, 2001; Bouldin et al., 2001; D'Angelo, 2009; Saboo & Kumar, 2016). Previous studies have reported relevance of all of the above-mentioned parameters for evaluating rutting resistance of bituminous binders, but comparison of these parameters with SBS and TPO modified bitumen is scarce and, hence, it is discussed in the present study.

3. Experimental program

Figure 1 shows the research methodology adopted for this study. Bituminous binders were subjected to conventional tests. After that advanced rheological tests were conducted which were comprised of rotational viscosity, temperature sweep test, and MSCR. For these tests, Brookfield viscometer model DV2T and TA instruments Dynamic Shear Rheometer (DSR) of Discovery HR-1 model were used. After rheological tests, morphology of bituminous binders was analysed with SEM, and chemical analysis was performed with FTIR tests. After finding out optimum SBS content as well as optimum TPO content in SBS modified binder, tests on strength characteristic were executed, which included Marshall Stability test and Indirect Tensile Strength. In the end, sixteen perpetual pavement sections with four types of layer combinations were designed and compared considering VG 30, VG 40 and SBS modified VG 30 binder with and without TPO as a bituminous layer.

3.1. Preparation of binders

TA high shear mixer, also known as a homogenizer, was employed for the blending of SBS and VG 30. A temperature of 160 °C and a stirring speed of 2000 rpm were maintained to ensure optimal compatibility and prevent polymer agglomeration. The mixing process persisted for 60 minutes to achieve thorough integration. For addition of TPO in SBS modified mix, the mixing temperature was kept at 140 °C to avoid TPO from aging.

3.1.1. Conventional tests

Penetration test helps grade the bituminous mix in terms of its hardness. The higher penetration value of the bitumen mixture shows softer consistency and vice-versa. Softening point of the bitumen mixture helps ascertain temperature sensitivity of the mixture. It indicates the tendency of mixture to flow at elevated temperature. It also helps in identifying temperature at which phase change occurs

in bituminous binder. Adhesive property of the bitumen along with its elasticity can be measured by ductility test. Ductile bitumen can form a thin ductile film around the aggregate particles. Thus, it does not crack at low temperatures. Insufficient ductility results in cracks when subjected to repeated traffic loads. Elastic recovery helps understand elastic capacity of binder from stress to recovery. Absolute viscosity is a measure of the resistance to flow. Higher viscosity bitumen means that more nearly it approaches a semi-solid state. The bitumen binders of low viscosity do not provide a uniform thin film for binding action but just lubricate the aggregate particles. Binders with high viscosity show heterogeneous character as full compaction is very difficult in this case. Hence, very high viscosity binders result in low stability values.

3.1.2. Temperature sweep test

Dynamic Shear Rheometer (DSR) testing, conducted in accordance with ASTM D 6373 (1999), was utilised for temperature testing. The continuous grade of the binder was determined as the temperature at which the rutting parameter reaches nearly 1.0 kPa under unaged conditions. This aids in identifying the high-temperature Performance Grade (PG) of the tested binders. The temperature range considered for measurements was 42 °C to 90 °C, with intervals of 6 °C, following the protocol outlined in AASHTO TP5 (1994). Testing was conducted at a frequency of 10 rad/s, with an oscillation strain of 12% and utilising 25 mm parallel plate geometry with a 1 mm gap setting. Samples were prepared using a circular silicon mould. Parameters such as complex shear modulus and phase angle were derived from this test.

3.1.3. Multiple stress creep and recovery test

MSCR test was conducted on both unmodified and modified binders following the guidelines outlined in ASTM D7405 (2015). The binder underwent testing at two stress levels: 0.1 kPa and 3.2 kPa. Previous research has highlighted a stronger correlation between the Jnr values estimated at 3.2 kPa and the rutting performance of bitumen mixes in both field and laboratory settings (White, 2017; Narayan et al., 2019).

The stress level of 0.1 kPa is chosen to maintain the bitumen within its linear viscoelastic range, thereby characterising its mechanical behaviour within that range. Conversely, the stress level of 3.2 kPa represents the bitumen in its non-linear viscoelastic range, providing insight into its mechanical behaviour in this non-linear range. Bituminous binders exhibiting lower values of Jnr are preferred for areas experiencing high traffic loads. The Jnr value measured at 3.2 kPa serves as a criterion for determining the suitability of the binder for different traffic categories, as illustrated in Table 6.

Table 6. Specification for Jnr value for different traffic level

Traffic Load	$J_{nr\ 3.2\ kPa,}$ kPa $^{-1}$	Details
Slow	2 to 4	10 million ESALs traffic
Heavy	1 to 2	10–30 million ESAL
Very Heavy	0.5 to 1	30 million ESALs traffic
Extremely Heavy	> 0.5	> 30 million ESALs traffic

3.1.4. Viscosity measurement

The test was conducted following the guidelines outlined in ASTM D4402 (2002) utilising a Brookfield viscometer. This test aims at determining the apparent viscosity of bitumen at elevated temperatures. A thermostatically controlled sample holder facilitates rotation, and torque measurements are utilised to gauge the relative resistance to rotation. The rotational speed and torque readings are subsequently employed to calculate the viscosity of the binder. Testing was carried out across a temperature range spanning from 120 °C to 180 °C, with a temperature difference of 15 °C between each measurement. Additionally, this test provides insights into the pumpability of the binder. The data derived from this test was further utilised for determining the mixing and compaction temperatures employing an equiviscous method.

3.1.5. Mixing and compaction temperature

3.1.5.1. Equiviscous or ASTM D 2493 method

In the equiviscous method, rotational viscosity is measured using a Brookfield viscometer at a shear rate of 6.8 s^{-1}, with the spindle submerged in the bituminous binder rotating at 20 rpm. The viscosity values obtained are plotted on a semi-logarithmic graph, from which the mixing temperature corresponding to 170 ± 20 mPa·s and the compaction temperature corresponding to 280 ± 30 mPa·s are determined. While this method helps standardise the effect of bitumen binder stiffness on mixture properties, it tends to yield higher temperatures for modified binders compared to conventional ones. This discrepancy arises because the ASTM D 2493 method is designed for base bitumen exhibiting Newtonian behaviour at high temperatures, whereas modified bitumen often demonstrates non-Newtonian behaviour. The resultant elevated temperatures, exacerbated by oxidation, can lead to bitumen hardening, emission, and odour issues. These viscosity-derived temperatures play a crucial role in altering the performance of mixtures. Given the lack of a universal method for selecting mixing and compaction temperatures for modified bitumen, many agencies have developed their own standards for estimating appropriate temperatures for each modified bitumen. This study also explores the utilisation of High Shear Viscosity (HSV) for determining mixing and compaction temperatures of modified bitumen.

3.1.5.2. High shear viscosity

Yildirim et al. (2000) noted that the shear rate applied in Superpave compaction surpassed that used in the ASTM D2493 method. To accurately determine viscosity at this shear rate for mixing and compaction temperature calculations, the Brookfield viscometer is employed. This entails measuring the viscosity of bitumen at various achievable shear rates, followed by plotting and extrapolating the data to a shear rate of 500 s^{-1}. The resultant viscosity values are then plotted on a semi-logarithmic graph, establishing the mixing temperature at 170 ± 20 mPa·s and the compaction temperature at 280 ± 30 mPa·s. In an attempt to achieve lower temperatures, the same authors suggest extending the viscosity range, proposing 275 ± 30 mPa·s for determining the mixing temperature and 550 ± 6 mPa·s for determining the compaction temperature.

3.1.6. Morphology and chemical characteristic

3.1.6.1. Scanning electron microscope (SEM)

The SEM analysis of all the binders was done by using EVO ZEISS MA15 instrument. SEM technology allows for the observation of bituminous mixes on a very small scale. It gives an idea about fracture and healing phenomenon in bituminous mixtures. It also helps in understanding dispersion of polymer or any other additive in bitumen. SEM can be used to decide on the compatibility or incompatibility of modifier material used to improve properties of bitumen. With observation at nanometre scales, SEM can help in detecting mini cracks in modified bitumen, which can assist engineers in decision making about the use of a particular material as a modifier in bitumen. SEM can help observe cohesion and adhesion within the binder and with other materials. The present study uses SEM technique to identify optimum content of SBS and TPO in bitumen.

3.1.6.2. The Fourier transform infrared spectroscopy (FTIR)

FTIR technique is used to observe components and consistency of bitumen modifiers. FTIR helps in understanding of functional groups of binders. It also assists in indicating change in chemical bonds in chemical reactions. The infrared spectra obtained from FTIR reflects the characteristic absorption peaks of virgin and modified bitumen. In the present study, infrared spectra of unmodified bitumen, SBS modified bitumen with and without TPO were obtained.

The FTIR spectra were recorded on a Shimadzu FTIR–8400 with the following specifications:

Light source: High brightness ceramic;
Beam Splitter: Germanium coated KBR plate;
Wavenumber: 400 to 4000 cm^{-1};
Resolution: 4 cm^{-1}.

3.2. Strength characteristics

3.2.1. Marshall stability test (MST) and indirect tensile strength (ITS) test

MST was conducted in accordance with ASTM D6927 (2016) specifications to determine the optimum binder content (OBC) for both modified and unmodified mixes. As per MoRTH guidelines (89), a binder content ranging from 5% to 5.8% was explored, with increments of 0.2%. Each mix comprised approximately 1200 g of aggregate with adopted gradation, blended with varying percentages of bitumen. Mixing occurred at predetermined temperatures, and the mixture was compacted in a pre-heated Marshall mould having a height of 63.5 mm and diameter of around 102 mm. Three samples were prepared for each binder content, compacted by applying 75 blows on both front and rear sides.

The Marshall stability value, representing the maximum load at failure, and flow value, indicating deformation, were determined as per ASTM D6927 guidelines. Compressive load was applied at a constant rate of 50 mm/min until specimen failure using the Marshall testing machine. Theoretical maximum specific gravity (Gmm) was determined for each sample, and subsequent analysis involved evaluating parameters such as bulk specific gravity (Gmb), percent air voids (Va), and density. Graphical plots were made for each parameter against different binder contents, with the binder content corresponding to 4% air voids selected as the OBC for the mix. The obtained parameters were checked against specified limits as per MoRTH guidelines.

The Indirect Tensile Strength (ITS) Test, conducted following ASTM D6931 (2017) procedures, aimed at determining the tensile strength of bituminous mixtures. This involved applying a load along the diametrical axis of cylindrical specimens at a fixed deformation rate of 5.1 cm/min until failure, with the total vertical load at failure recorded at 25 °C. Higher ITS values indicate improved resistance to fatigue cracking and deformation, offering insights into the adhesion test among aggregate and bitumen. During testing, it was ensured that two loading strips remained parallel to each other.

The ITS is calculated by the following equation:

$$\mathrm{ITS} = 2P/\pi td, \tag{1}$$

where P = maximum load carried by the specimen up to the failure, KN; t = specimen thickness, cm; d = specimen diameter, cm.

The indirect tensile strength test serves as a valuable tool for evaluating the tensile properties of bituminous mixes, offering insights that can be correlated with pavement cracking. A higher value of indirect tensile strength indicates greater resistance to low temperature cracking, highlighting the mix's ability to withstand tensile strains prior to cracking.

Additionally, the tensile strength ratio (TSR), calculated using Equation (2), provides an indication of the mix's moisture resistance capability. A higher TSR value is preferred as it signifies better resistance to moisture damage.

$$TSR = 100(S1/S2), \quad (2)$$

where S1 = ITS value of conditioned specimens, kPa; S2 = ITS value of unconditioned specimens, kPa.

4. Results and discussion

4.1. Conventional tests

The notation used to distinguish between different mixes in this study is outlined in Table 7, which also summarises the results of conventional tests. An increase in SBS dosage led to elevated softening point and viscosity. However, the addition of TPO in SBS modified bitumen resulted in a decrease in softening point, thereby enhancing the consistency and temperature sensitivity of SBS modified bitumen.

Furthermore, augmenting SBS dosage decreased penetration value, indicating increased stiffness. Conversely, the incorporation of TPO in SBS modified bitumen increased penetration value, signifying an enhancement in binder consistency. This increased consistency is advantageous for the low-temperature properties of SBS modified bitumen. The addition of SBS heightened the viscosity of the base binder, whereas TPO addition in SBS modified bitumen reduced it. Moreover, ductility and elastic recovery of the binder increased with higher SBS content, indicating improved low-temperature performance. The addition of TPO resulted in a further increase in ductility and elastic recovery of SBS modified bitumen.

Table 7. Basic characterisation of modified binders

Mix	Binder ID	Penetration at 25 °C	Softening Point, °C	Ductility, cm	Elastic Recovery	Specific Gravity	Viscosity (poise) @60 °C
VG 30+ 1% SBS	S1	50	51	93	50	0.99	2580
VG 30+ 2% SBS	S2	48	56	91	57	0.99	2620
VG 30+ 3% SBS	S3	46	60	90	64	1.00	2910
VG 30+4% SBS	S4	45	63	88	66	1.00	3110
VG 30+ 3% SBS+1% TPO	S3/T1	48	58	92	69	0.99	2860
VG 30+ 3% SBS+2 % TPO	S3/T2	49	55	94	71	0.99	2590
VG 30+ 3% SBS+3 % TPO	S3/T3	52	52	97	72	0.99	2470

4.2. Rheological performance

4.2.1. Superpave performance grade (PG)

PG grading of bituminous binders is expressed in terms of high and low temperatures at which they are expected to perform satisfactorily. For this purpose, samples are tested at high as well as low temperatures regimes with the help of DSR. However, in the present study, investigations are limited to high temperature regimes only as the average annual temperature in most part of India is around 35 °C. According to SHRP method, superpave rutting parameter value should be less than 1.0 kPa for unaged binder.

From the test results, it can be observed that VG 30 (PG 64-XX) when modified with SBS and then with optimum content of SBS with addition of TPO shows behaviour similar to PG 70. Figure 2 illustrates the high temperature PG determined for unmodified and modified bitumen. It can be observed that continuous grade increased because of SBS as well as TPO addition in VG 30 binder. S3/T1 and S4 showed a considerable increase and performed better than hard binder VG 40 whereas S3 binder performed equally to VG 40. The sequence of high temperature PG grade performance was S4 > VG 40 > S3 > S3/T1 > S3/T2 > S2 > S3/T3 > S1 > VG 30.

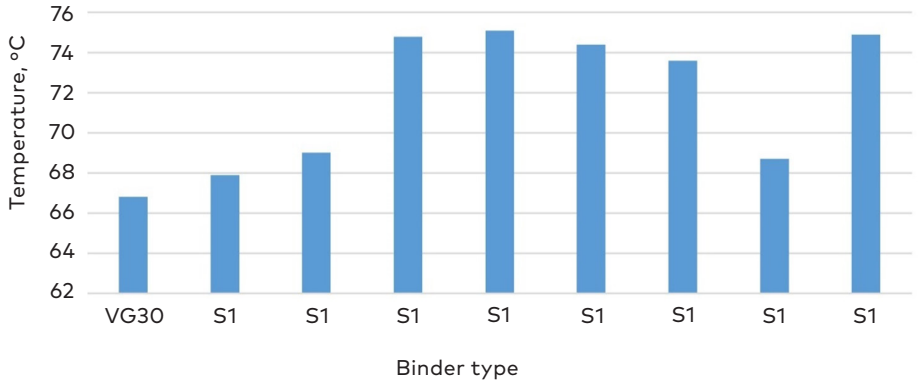

Figure 2. High temperature PG of various binders

4.2.2. Superpave performance grade (PG)

The phase angle δ of all binders, except for TPO modified bitumen, increased with rising temperature. The phase angle serves as an indicator of viscoelastic characteristics, with higher δ values indicating a greater proportion of viscosity. Interestingly, TPO-added SBS modified bitumen exhibited relatively lower δ values at higher temperatures. The G^* value reflects the binder's resistance to deformation under repeated shear, where higher G^* values signify better resistance to shear deformation. However, due to poor deformation resistance of bitumen at high temperatures, G^* values decrease with increasing temperature. Figure 3 illustrates the performance comparison at 60 °C, which closely approximates the maximum temperature experienced in many parts of India. Binders S3 and S3/T1 demonstrated superior performance compared to base bitumen VG 30 at this temperature. Particularly, binder S3 outperformed VG 40 bitumen. At 60 °C, the sequence of deformation resistance, based on performance, was VG 40 > S3 > S4 > S3/T1 > S3/T2 > S2 > S1 > VG 30 > S3/T3. It is notable that G^* values decrease and δ values increase for all virgin and SBS modified bitumen with increasing temperature.

Polymer-modified bitumen binders generally exhibit higher G^* and lower δ values, indicating they are typically stiffer and more elastic compared to unmodified bitumen. This behaviour is attributed to the effect of high temperature on the cohesion properties of bitumen, resulting in lower stiffness and a more viscous nature.

There are various potential explanations for the decrease in G^* and PG temperature upon the inclusion of TPO in bitumen. One possibility is that TPO

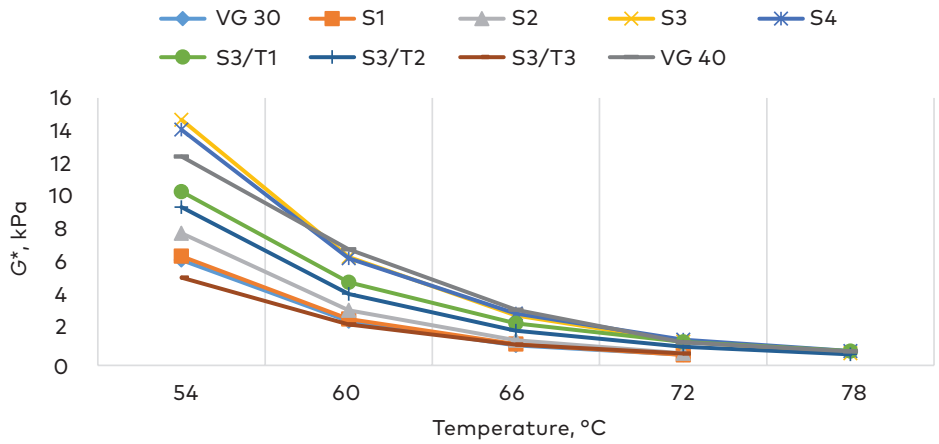

Figure 3. *G** vs. temperature

modifies the molecular structure of bitumen, leading to alterations in its rheological properties. For instance, TPO may disrupt the organisation of bitumen molecules, resulting in decreased stiffness and increased flexibility, consequently lowering the G^*/PG temperature. Another possibility is that TPO may influence the surface properties of bitumen, such as surface energy or roughness, thereby affecting its rheological behaviour and decreasing the G^*/PG temperature.

The addition of TPO in SBS modified bitumen resulted in a significant decrease in δ value, as depicted in Figure 4. This is attributed to TPO interacting with bitumen and reducing stiffness. When tire pyro oil is introduced into a bituminous binder, it functions as a viscosity reducer and plasticizer, rendering the binder more flexible and less viscous. Consequently, this reduces the complex shear modulus and phase angle of the binder. The mechanism underlying the reduction in complex shear modulus and phase angle of the binder by tire pyro oil is believed to be linked to its chemical composition and molecular structure. Tire pyro oil, derived from the tire recycling process, comprises a complex mixture of organic and inorganic compounds. Some of these compounds, like polycyclic aromatic hydrocarbons, are known to have viscosity-reducing and plasticizing effects on bitumen. They interact with bitumen molecules, altering their structure and organisation, thereby reducing the complex shear modulus and phase angle of the binder. Furthermore, tire pyro oil contains other compounds that can influence bitumen properties. For instance, it contains low levels of sulphur, which can enhance the stability and rheological properties of the binder. Additionally, it contains trace amounts of metals and other inorganic compounds, acting as catalysts to improve oxidation and aging resistance of the binder. Based on δ value performance at 60 °C, the sequence of binders ranked from best to least performing was S3/T1 > S3/T2 > S3/T3 > S4 > S3 > VG 40 > S2 > S1 > VG 30.

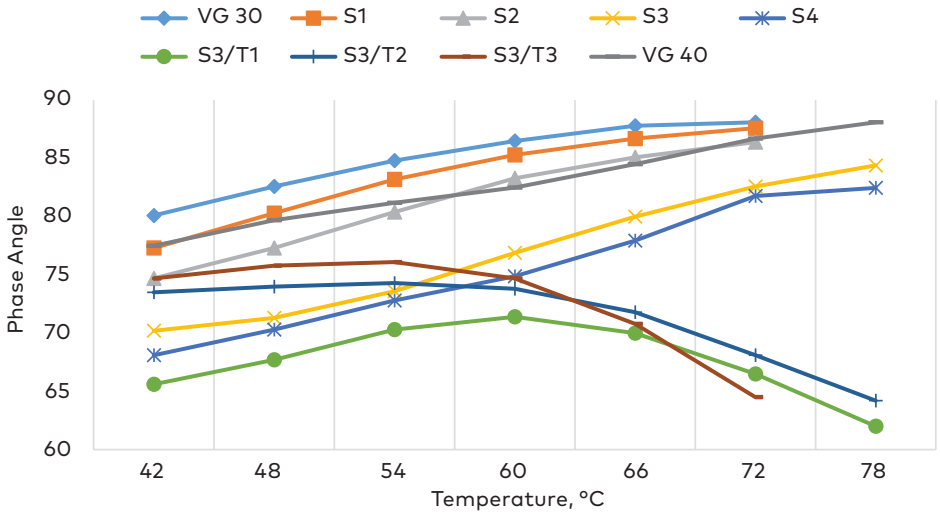

Figure 4. Phase angle vs. temperature

The parameter tanδ serves as an indicator of the viscoelastic behaviour of bitumen. It is particularly sensitive to changes in the phase angle, especially at higher values of δ. Tanδ represents the ratio of the viscous component to the elastic component. Upon analysis of the tanδ parameter, it was observed that the parameter value of the SBS modified binder increased compared to the base bitumen. TPO modified binder showed negligible change. Prominent difference is observed after 48 °C. After this viscous behaviour of VG 30 is characterised by the higher value of tanδ. From Figure 5, it can be seen that modified binders have milder gradient than base bitumen which indicates a lower thermal sensitivity of modified binders. The ranking of binders as per performance with respect to parameter tanδ is similar to the ranking discussed in δ parameter. The anti-rutting factor or superpave rutting parameter $G^*/\sin\delta$ of modified bitumen was tested as explained earlier. It was observed that modified binders had higher values of $G^*/\sin\delta$ than unmodified binders. High temperature rutting resistance is better if superpave rutting parameter is higher.

As depicted in Figure 6, the $G^*/\sin\delta$ parameter decreases with an increase in temperature. Additionally, SBS and TPO modifications enhance the $G^*/\sin\delta$ parameter of the binder, thereby improving high-temperature rutting resistance. One possible explanation for this improvement is that SBS and TPO enhance the elastic behaviour of the binder, leading to an increase in the $G^*/\sin\delta$ parameter. SBS, being a type of rubber, can augment the binder's elasticity, while TPO, an oil, can mitigate its viscous behaviour. Both modifications contribute to an increase in the $G^*/\sin\delta$ parameter, which measures the binder's ability to deform and recover under stress. This suggests that the modified VG 30 binder is stiffer than the unmodified

one. At 60 °C, with the exception of the S3/T3 binder, all other binders outperformed VG 30. At 60 °C, sequence of performance as per rut factor was VG 40 > S3 > S4 > S3/T1 > S3/T2 > S2 > S1 > VG 30 > S3/T3. Improved rutting factor $G^*/\sin\delta$[9] and non-recoverable compliance (Shenoy parameter) were also determined to evaluate and compare high temperature performance of all bituminous binders.

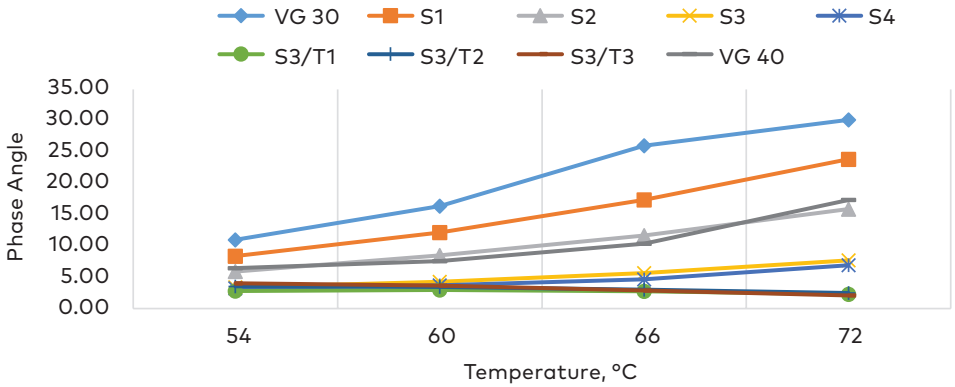

Figure 5. tanδ vs. temperature

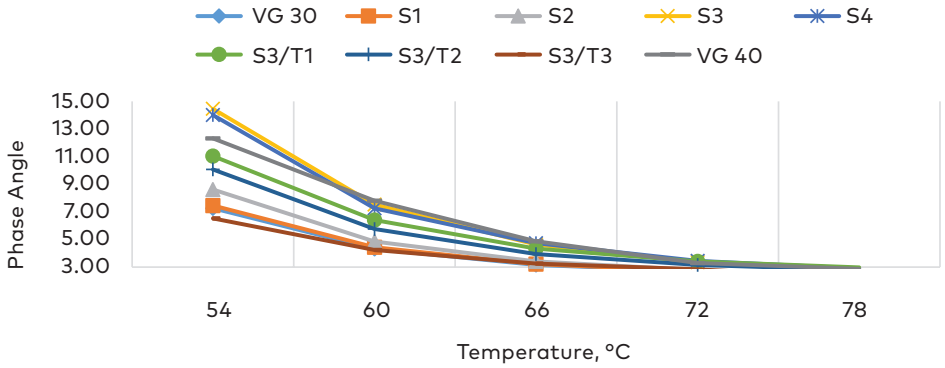

Figure 6. Superpave rutting parameter at various temperatures

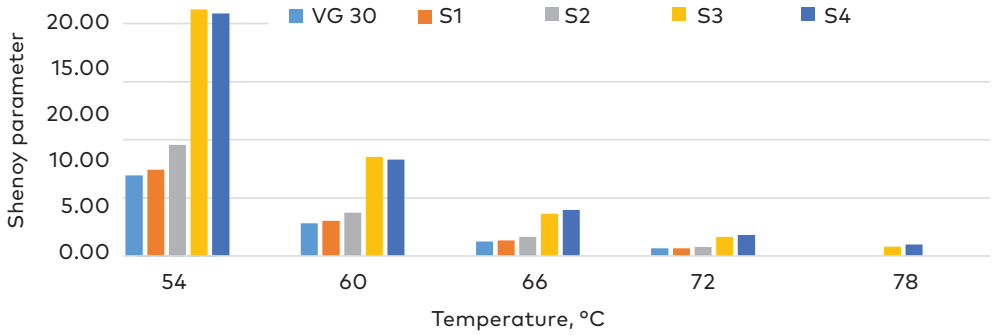

Figure 7. Shenoy parameter

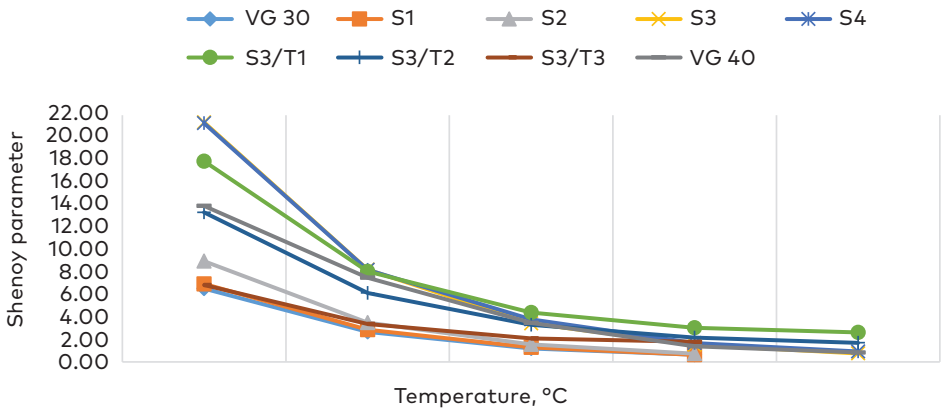

Figure 8. $G^*/Sin\delta^9$ vs. temperature

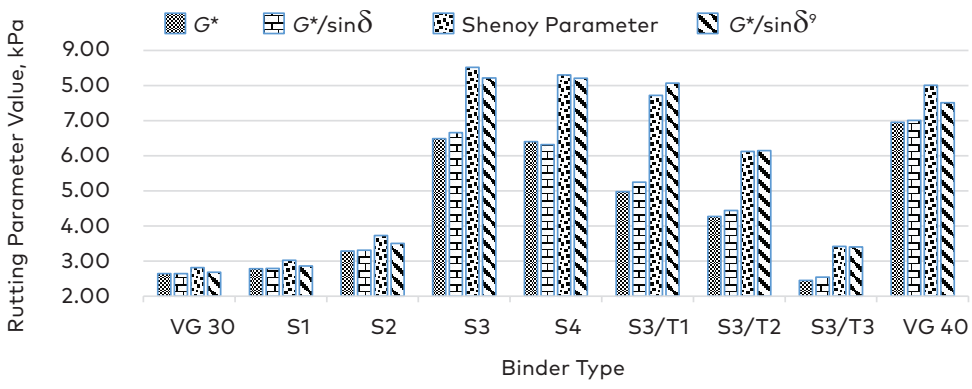

Figure 9. Comparison of various rutting parameters at 60 °C

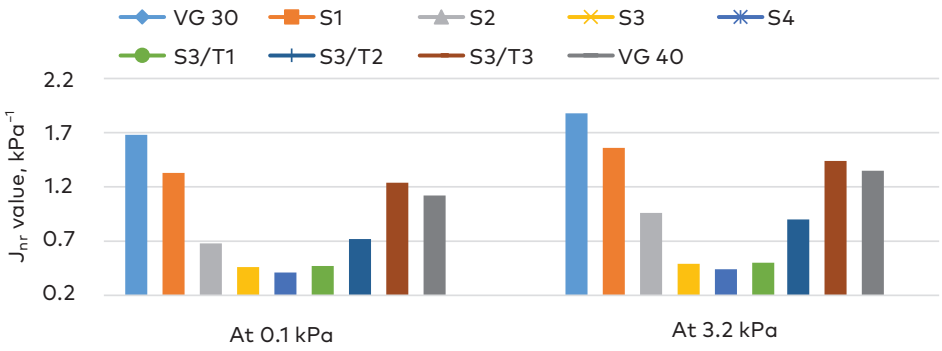

Figure 10. MSCR parameter

Figure 7 describes the variation in Shenoy parameter for unmodified and modified binders at different temperatures. An increase in Shenoy parameter indicates higher rutting resistance. The ranking as per Shenoy parameter performance at 60 °C is S3 > S4 > VG 40 > S3/T1 > S3/T2 > S2 > S3/T3 > S1 > VG 30. Overall, the ranking suggests that the SBS and TPO modified binders have improved rheological properties compared to the VG30 binder. Figure 8 shows the sequence of performance at 60 °C, as per the improved rutting factor $G^*/\sin\delta$[9] is S3 > S4 > S3/T1 > VG 40 > S3/T2 > S2 > S3/T3 > S1 > VG 30. Figure 9 shows comparison of all the rutting factors as discussed above at 60 °C. It can be seen that Shenoy parameter and improved rutting factor gives higher values for modified binders. The evaluation results of $G^*/\sin\delta$ differed from the improved rutting factor $G^*/\sin\delta$[9], which may be attributed to the actual rutting of bituminous pavement occurring in the nonlinear viscoelastic deformation range of the bitumen binder. Additionally, $G^*/\sin\delta$ reflects the mechanical property of materials under undamaged conditions, serving as an evaluation parameter when the bitumen is in the linear viscoelastic range.

4.2.3. Multiple stress creep recovery test (MSCR))

MSCR tests were conducted at 1 kPa and 3.2 kPa stress levels, focusing solely on 60 °C temperature to replicate high service temperature conditions in India. Lower Jnr values indicate higher rut resistance in bituminous binder. The test utilised 25 mm parallel plate geometry with a stress duration of 1 s followed by a 9-second recovery period. Figure 10 compares the Jnr obtained from MCSR tests at 3.2 kPa and 1 kPa. Modified binders demonstrated lower Jnr values than the base binder, signifying improved resistance to permanent deformation. Notably, SBS

modified bitumen exhibited the lowest values compared to both VG 30 and VG 40. This suggests that VG 30 may not be suitable for very heavy or extremely heavy traffic loads, while VG 40, S3/T1, and S3/T2 binders are suitable for such conditions. Binders like S1 and S2 are deemed useful for very heavy loads, whereas S3 and S3/T1 are more appropriate for extremely heavy loads. Modification with SBS and TPO can enhance binder grades. The performance ranking in this test is summarised as follows: S4 > S3 > S3/T1 > S2 > S3/T2 > VG 40 > S3/T3 > S1 > VG 30. Table 8 outlines rut resistance rankings for all examined binders, ranging from 1 to 9, with a rank of 9 indicating the lowest rut resistance and rank 1 the highest. Binder S3 demonstrates superior performance among other SBS-modified binders, with binder S3/T1 surpassing all other SBS-modified binders with TPO addition. These findings suggest that modified binders not only enhance VG 30 quality but also surpass VG 40 in rutting resistance. Thus, TPO+SBS modified bitumen emerges as a promising solution for high-temperature bitumen applications, highlighting the efficacy of TPO as a viable option for bitumen modification, especially in conjunction with polymers like SBS.

Table 8. Ranking of binders as per various performance parameters at 60 °C

Sr. No	Binder ID	PG Grade	G^*	δ	$G^*/\sin\delta$	$G^*/\sin\delta^9$	Shenoy parameter	J_{nr}
1	VG 30	9	8	9	9	9	9	9
2	S1	8	7	8	7	8	8	6
3	S2	6	6	7	6	6	6	4
4	S3	3	2	5	2	1	1	2
5	S4	1	3	4	3	2	2	1
6	S3/T1	4	4	1	4	3	4	3
7	S3/T2	5	5	2	5	5	5	5
8	S3/T3	7	9	3	8	7	7	8
9	VG/40	2	1	6	1	4	3	7

4.3. Morphology and chemical analysis

4.3.1. SEM analysis

The SEM technique is employed to examine morphology and evaluate modifier distribution in bitumen samples. Figure 11 displays SEM images for each sample. The base asphalt exhibits a homogeneous morphology with a slightly wrinkled surface. However, SEM images of SBS-modified asphalt reveal polymer dispersion within the base asphalt. Upon addition of SBS to bitumen, it absorbs the low molecular oil fraction of the bitumen, resulting in heterogeneous morphologies in

the SEM images of SBS-modified samples. SEM image shows dispersed polymer rich phase as bright and continuos asphaltene phase as dark. In case of S1 and S2, the asphalt is continuos phase and polymer phase is dispersed through it, also microstructure appers to be forming in case of S2. In case of S3, better dispersion of the polymer is observed. In S3, polymer content is high enough for polymer to be the matix of the system as a continuos polymer phase stabilises the network between base bitumen and polymer. SBS starts to become the dominent phase at 4% SBS. The higher SBS concentration indicates incompatibility at this dosage. Extensive spreding of polymer particles may lead to a decrease in engineering properties of bitumen. In case of TPO addition in S3, S3/T1 sample clearly shows better dispersion of polymer and oil. SEM image of S3/T2 and S3/T3 shows that dispersed TPO phase, which is clearly darker than asphaltene phase, is dominant and may lead to a decrease in performance of S3 binder.

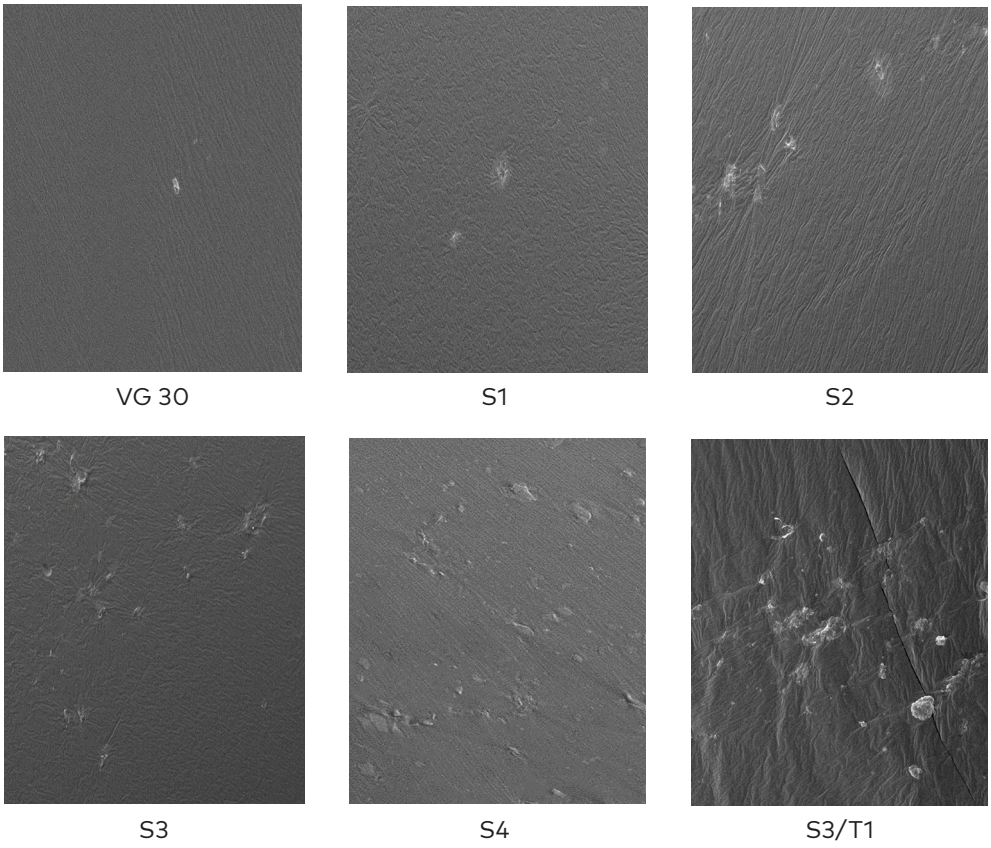

Figure 11. SEM images of binders (figure continues on the next page)

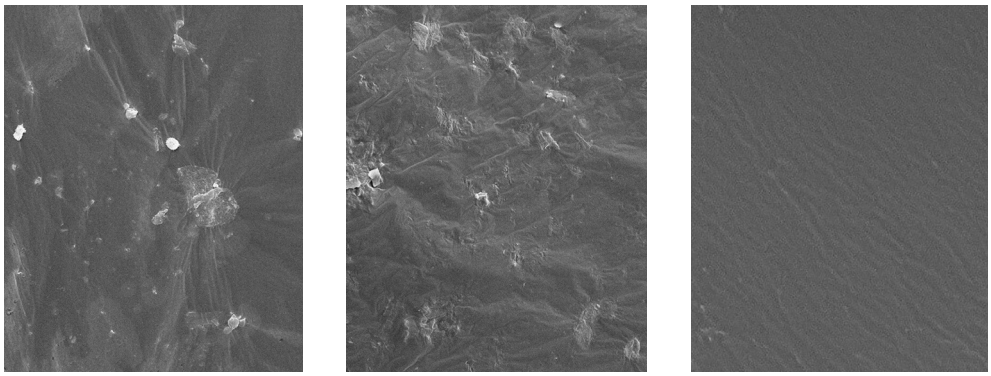

Figure 11. SEM images of binders

4.3.2. FTIR test

FTIR spectra of SBS modified samples were similar; hence, only graph of S3 is shown here. Also, spectra of SBS modified TPO added samples were similar; hence, only graph of S3/T1 is shown here along with spectra of VG 30 base bitumen and TPO as shown in Figure 12. The graphs of wave numbers ranging from 4000 cm^{-1} to 500 cm^{-1} were included in the spectrums. There was not any characteristic peak in the region between 4000 cm^{-1} to 3000 cm^{-1}. The characteristic peaks are concentrated near 2920 cm^{-1}, 2850 cm^{-1}, 1455 cm^{-1}. In the spectrum, the peaks within 2800–3000 cm^{-1} are typical C-H stretching vibration in aliphatic chains. The peak at 1454 cm^{-1}, 1455 cm^{-1} and 1456 cm^{-1} is related to C=C stretching vibration in aromatics. In case of unmodified and modified bitumen, the C-H symmetric deforming in C-H3 is observed at 2850 cm^{-1} whereas C-H asymmetric deforming in C-H3 is observed at around 1456 cm^{-1}. The appearance of absorption peak at 2142 cm^{-1}, 2184 cm^{-1} and 2212 cm^{-1} shows presence C ≡ C.

The wavenumber of around 1600 cm^{-1} is related to stretching vibrations of the C=C double bond of aromatics. The peak at 723 cm^{-1} shows the presence of molecules with more than four carbon atoms in a row. In case of all SBS modified bitumen, there is a new peak at 956 cm^{-1} and in S3/T1 it is at round 965 cm^{-1} which is related to the bending vibration of C-H in the butadiene bonds -CH=CH-. The new peak in S3/T1 at 1159 cm^{-1} indicates C-O stretching vibrations peak due to addition of TPO. The spectral region from 500 cm^{-1} to 1400 cm^{-1} is referred to as Finger Print Region. This region exhibits many complex bands with overlapping in nature. This is the most complex part of the spectrum and contains a number of absorption bands which appear due to skeletal stretching and bending vibrations. Even though this region is not useful for interpretation, it is helpful for sample comparison. As we are

dealing with complex matrix, the appearance of slightly different peak scan cannot be assigned to any probable suggestive structure. The results shown in Figure 12 suggest that the obtained mix is homogenous. It can also be concluded that the SBS modified bitumen causes only physical modification as there is no new major peak or shift in peak position (Masson et al., 2003).

Table 9. FTIR analysis of TPO

Wave number cm^{-1}	Bonds	Class of compounds	Bonds	Class of compounds
748.65	C- Cl	Chloride	C=C stretching	Alkenes
1373.46	Nitrate	Nitrate	C-H bending	Alkanes
1454.78	O-H, Bending	Alcohol	Carbon-carbon stretching	Aromatic compounds
1599.62	C=C, C=N, Stretch	Alkenes, Amide	C=C stretching	Alkenes
2850.48	C-H, Stretch	Alkanes	C-H stretching	Alkanes
2919.21	C-H, Stretch	Alkanes	C=C stretching	Alkenes

The FTIR analysis of TPO reveals that the functional groups present are primarily aromatics and hydrocarbons, as shown in Table 9. The compounds in light TPO include alkanes, alkenes, and aromatic compounds. The pyro oil spectra exhibit additional peaks beyond 3000 cm^{-1} (O-H stretch), representing the alcohol functionalities. From Figure 12, it can be observed that no significant new peaks emerged after the addition of pyro oil in the modified bitumen, suggesting the absence of new functionalities in the modified bitumen. However, several shifts in peaks are observed in the spectra of S3/T1. For instance, the peaks at 2033 cm^{-1} and 2184 cm^{-1} shift left to 2214 cm^{-1} and 2162 cm^{-1}, respectively, after modification with TPO. The FTIR spectra of TPO reveal the presence of fats, acids, alkanes, ethers, etc. in TPO. These components in TPO, when compared to bitumen, have relatively lower molecular weights. The lighter components present in TPO aid in blending, modifying the chemical composition of bitumen and improving its technical performance (Chen et al., 2022). It is noteworthy that during the preparation of TPO-modified bitumen, no new chemical functional groups are generated, and there are no chemical reactions occurring in the preparation process.

Based on the conventional, rheological and morphological test results, it was concluded that 3% SBS was the optimum content for SBS modification of VG 30 bitumen whereas 1% TPO was optimum content of oil in modified VG 30 with 3% SBS. To compare strength characteristics of modified binder with optimum content of SBS with and without addition of TPO, Marshall stability and ITS tests were done on VG 30, S3, S3/T1 and VG 40 binders. In the following part, FTIR indices are discussed.

To analyse the effect of oxidation due to the modification process on the binders, the carbonyl and sulphoxide indices are calculated by using the following equations:

Carbonyl Index: $I_{C=0} = \frac{A_{1700}}{\sum A}$

Sulphoxide Index: $I_{S=0} = \frac{A_{1030}}{\sum A}$

where, A_{1700} = area of spectral band around 1700 cm^{-1};

A_{1030} = area of spectral band around 1030 cm^{-1};

$\sum A$ = total area of spectral bands between 2000 to 600 cm^{-1}.

The carbonyl index (I_C=O) and sulphoxide index (I_S=O) serve as indicators of the concentration of carbonyl and sulphoxide functional groups in a chemical compound, respectively. These functional groups, prevalent in numerous organic compounds, are typically distinguished by the presence of a carbon atom double-bonded to an oxygen atom (C=O) for carbonyls and a sulphur atom double-bonded to an oxygen atom (S=O) for sulphoxides. The carbonyl and sulphoxide indices are often used to characterise the chemical composition of various materials, such as polymers, fuels, and foods. They can provide information on the presence and concentration of functional groups in a compound, which can be useful for understanding its chemical properties and reactivity.

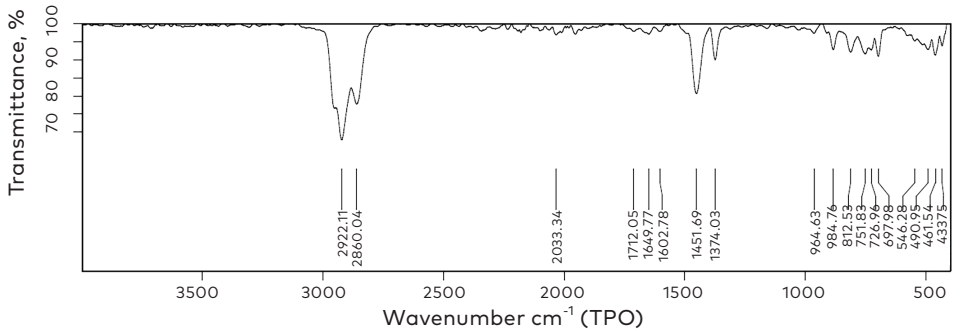

Figure 12. FTIR test on TPO, modified & unmodified binder (figure continues on the next page)

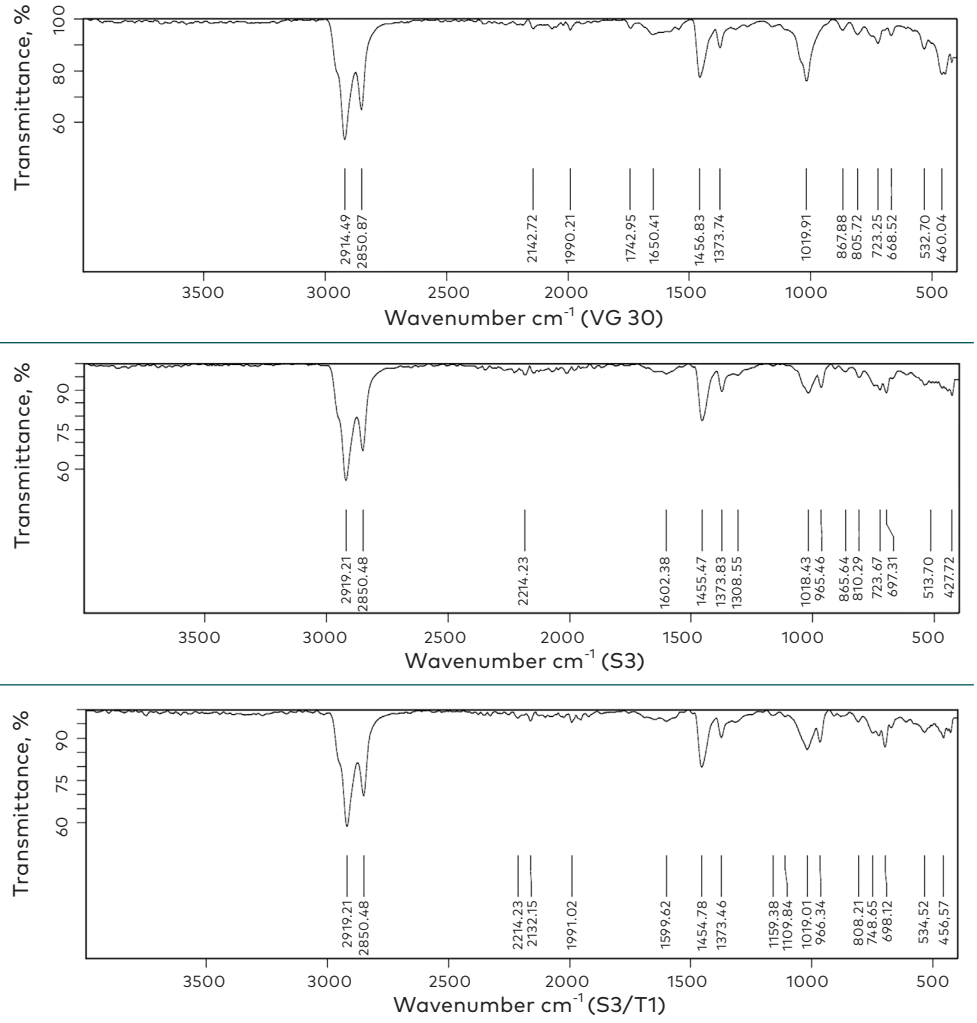

Figure 12. FTIR test on TPO, modified & unmodified binder

Figure 13 shows the carbonyl and sulphoxide indices for the base and SBS modified binders. From the figures it can be observed that the carbonyl index increased for S3T1 after addition of TPO in S3. This may be because of the high amount of carbon present in the TPO, and also may be due to the higher carbonyl groups in the TPO. On the other hand, the sulphoxide index of S3T1 is found to be minimum after modification. This may be because of the absence of sulphoxide functional groups.

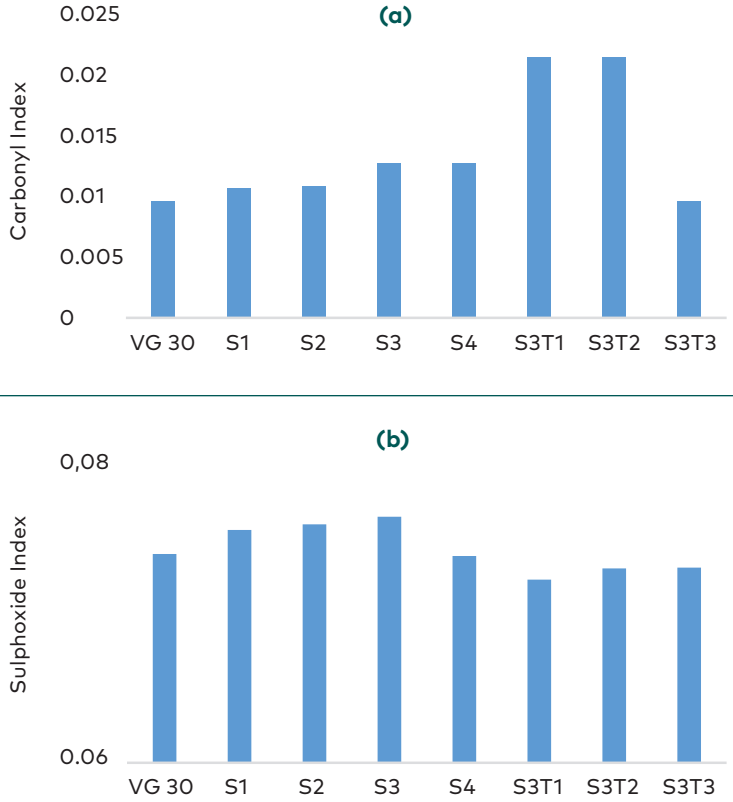

Figure 13. Carbonyl and sulphoxide indices

Figure 14 illustrates the correlation between the carbonyl index and $G^*/\sin\delta$ values for the base, SBS-modified, and S3+TPO-modified binders. The X-axis represents the carbonyl index, while the Y-axis depicts the $G^*/\sin\delta$ values at 60 °C. A strong correlation is evident with coefficients of determination of 0.93 and 0.92 for the base and modified binders, respectively. A positive linear relationship is observed between the carbonyl index and rutting factor. This suggests that incorporating SBS and TPO into the base binder enhances its rutting resistance by elevating the carbonyl index. The carbonyl index serves as a measure of unsaturated bonds in bituminous binder, which are believed to bolster rutting resistance by facilitating energy dissipation through bond formation during deformation. Consequently, higher carbonyl index values correspond to improved rutting resistance, indicating greater resistance to rutting with an increased carbonyl index.

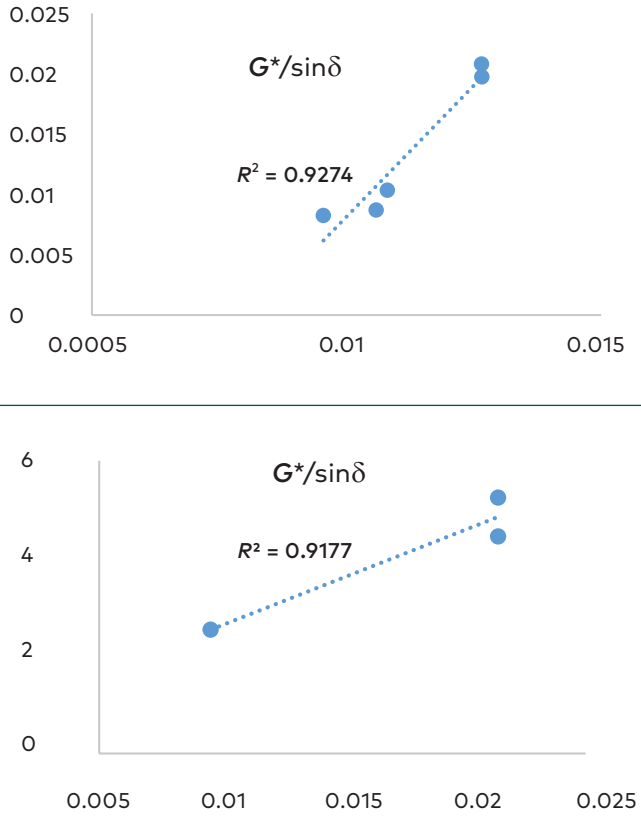

Figure 14. Correlation between the carbonyl index and G*/sinδ

4.4. Mixing and compaction temperature

The equiviscous method was employed to determine the mixing and compaction temperatures of both modified and unmodified binders, involving viscosity measurements at 135 °C, 150 °C, and 165 °C. Subsequently, the viscosity values were plotted on a conventional log-log temperature graph to ascertain the mixing and compaction temperatures, set at 170 ± 20 mPa·s and 280 ± 30 mPa·s, respectively. Table 10 presents the results obtained from this method. It is notable that while the equiviscous method provides reasonable mixing and compaction temperatures for the base bitumen, it yields considerably higher values for SBS-modified binders due to increased viscosity. Such elevated temperatures may lead to polymer degradation, particularly as temperatures exceeding 180 °C are generally discouraged (Cortizo et al., 2004). Because extreme high temperature may result in hardening due to

volatilization and oxidation. In addition, such high temperatures cause problems like excessive lateral movement of mix during rolling, excess absorption of bitumen in aggregates which results in lower effective bitumen binder content and high in-place air voids.

Table 10. Mixing and compaction temperature range

Binder	ASTM D 2493		HSV	
	Mixing, °C	Compaction, °C	Mixing, °C	Compaction, °C
VG 30	150–155	147–152	-	-
S3	176–179	166–171	162–165	155–158
S3/T1	167–170	160–163	156–159	149–152
VG 40	152–157	144–149	-	-

Trying to get lower mixing and compaction temperature for modified binders, HSR method was adopted. The method is similar to ASTM D 2493, but in HSR, shear rate value is around 500 s^{-1} instead of 6.8 s^{-1}. Similar to equiviscous method, viscosity values were plotted to determine mixing and compaction temperature. The temperatures obtained by HSR method were clearly lower than the eqiviscous method as shown in Table 10. Addition of TPO in SBS modified binder reduces the mixing and compaction temperature. The reduction in temperature is attributed to lower viscosity value used. Modified bitumen shows a non-Newtonian behaviour in which an increase in shear rate results in lower viscosity values.

4.5. Marshall method and ITS test

A total of 60 specimens, three for each binder type and binder content, were prepared to determine the optimum binder content (OBC) for both unmodified and modified bitumen. All specimens were fabricated using mixing and compaction temperatures obtained from Table 10. The loose mixtures exhibited Gmm values within the range of 2.45–2.55, while the bulk density of compacted samples ranged from 2.38–2.4 g/cc. Voids in mineral aggregates exceeded the minimum requirement of 13% for all samples, with air voids ranging from 3.44–5.54% and showing a decreasing trend with increasing bitumen content. Meanwhile, the voids filled with asphalt ranged from 65.31–77.15% across all samples, showing an increasing trend with bitumen content.

Table 11 summarises the findings regarding OBC, indicating that the OBC for SBS-modified binder is higher compared to unmodified binder due to the higher viscosity of the former. Increased SBS content leads to higher viscosity, requiring a greater quantity of binder for aggregate coating. Conversely, with TPO modification, the OBC value decreases as viscosity reduces due to the presence of oil. The Marshall

stability values for each mix type, averaged over three specimens, are also presented in Table 11. Notably, the OBC for SBS-modified bitumen is higher than that for VG 30 due to its increased viscosity, while the addition of TPO decreases the OBC value from 5.4% to 5.2% due to reduced viscosity from the presence of oil. The Marshall stability value of SBS-modified binders, with and without TPO, exceeds that of VG 30 due to increased viscosity, confirming that a stiffer binder results in higher stability.

Furthermore, the conditioning process leads to a decrease in stability value, as water can disrupt the cohesion and stiffness of the bitumen-aggregate interface. The Indirect Tensile Strength (ITS) test, conducted on both unconditioned and conditioned samples, involved soaking the specimens in a water bath for 60 min at 35 °C, as per IRC 37 guidelines, and then testing them after conditioning for 24 h at 60 °C. The peak load at failure was recorded to calculate the ITS value of each specimen. Table 11 also displays the results of the ITS test, indicating that all binders met the minimum criteria of 80% TSR ratio.

Table 11. Performance evaluation of binders

Test	Details	VG 30	S3	S3/T1	VG 40
Marshall Stability	OBC, % by wt. of mix	5.2	5.6	5.4	5.4
	Unconditioned, KN	13.88	21.20	20.50	21.93
	Conditioned, KN	12.17	20.89	19.49	19.10
ITS	Unconditioned, kPa	792	1120	1067	1641
	Conditioned, kPa	710	984	949	1396
	TSR	89.64	87.85	88.94	85.12
Resilient Modulus	Mr, MPa	2000	2512	2408	3000

5. Perpetual pavement design and comparison with respect to life cycle cost and carbon dioxide emission

To estimate the Resilient Modulus (Mr) of a modified binder at 35 °C without specific testing facilities, an empirical formula recommended by IRC 37 guidelines (1) can be employed.

$$Mr = 1170 + (1.991 \times ITS), \quad (3)$$

where

ITS = Indirect Tensile Strength in kPa; Mr = Resilient Modulus, MPa.

The resilient modulus values for the binders tested in the ITS test are derived from Equation (3). An analysis of Table 12 reveals that the modified bituminous binder exhibits a higher resilient modulus. Additionally, the addition of TPO in SBS modified bitumen results in a reduction of the resilient modulus of S3 by only 4%,

although it remains higher than that of VG 30. One of the objectives of this study was to suggest bituminous mixtures with modified VG 30 to address availability issues of VG 40. Hence, it is important to compare the pavement designs with modified and unmodified bitumen to check whether satisfactory results are observed. The summary of material properties like Poison's ratio and resilient modulus, considered for pavement design in the present study are shown in Table 12.

Table 12. Material properties considered as per the guidelines in IRC 37:2018

Material Type	Poisson's ratio	Elastic/Resilient Modulus, MPa
Granular base over sub-base treated with cement	0.35	350
Subgrade	0.35	$17.6 \times (CBR)^{0.64}$
Unbound granular layers	0.35	$0.2 \times M_{RS} \times (h)^{0.45}$
Sub-base treated with cement	0.25	600
Aggregate Interlayer	0.35	450
Bituminous layer with VG 40 binder	0.35	3000
Bituminous layer with VG 30 binder	0.35	3000

Table 13. Combinations for perpetual pavement

Binder Used	Combination details for design of pavement	ID
VG30	BL+WMM+GSB	A
	BL+GSB	B
	BL+CTSB+GSB	C
	BL+ AIL+CTB+GSB	D
S3	BL+WMM+GSB	E
	BL+GSB	F
	BL+CTSB+GSB	G
	BL+ AIL+CTB+GSB	H
S3/T1	BL+WMM+GSB	I
	BL+GSB	J
	BL+CTSB+GSB	K
	BL+ AIL+CTB+GSB	L
VG40	BL+WMM+GSB	M
	BL+GSB	N
	BL+CTSB+GSB	O
	BL+ AIL+CTB+GSB	P

Table 14. Thickness of different perpetual pavement trial combinations

Combination	Pavement layers with thickness, mm					Total thickness, mm	Horizontal tensile strain, μs	Vertical compressive strain, μs
Combination A								
	GSB	WMM	DBM		BC			
A	200	150	310		50	710	80.00	155.20
E	200	150	280		50	680	79.43	157.70
I	200	150	285		50	685	79.75	157.40
M	200	150	255		50	655	79.64	161.80
Combination B								
	GSB		DBM		BC			
B	200		340		50	590	79.12	179.70
F	200		305		50	555	78.78	182.90
J	200		310		50	560	79.32	183.20
N	200		275		50	525	79.93	189.50
Combination C								
	CTSB	WMM	DBM		BC			
C	200	150	250		50	650	79.96	168.10
G	200	150	230		50	630	78.34	168.20
K	200	150	235		50	635	78.22	167.30
O	200	150	210		50	610	78.53	171.90
Combination D								
	GSB	CTB	AIL	DBM	BC			
D	200	100	100	205	50	655	78.82	137.20
H	200	100	100	185	50	635	78.90	139.20
L	200	100	100	170	50	640	78.38	144.10
P	200	100	100	150	50	600	80.00	171.40

Bituminous layer is composed of DBM + 50 mm bituminous concrete layer. As per IRC 37 guidelines, bituminous base and surfacing course are considered as a single layer. In this study, minimum thickness permissible for layers except BL as per IRC 37 guidelines is considered for all the trial sections as shown in Figure 15. Table 13 provides the nomenclature used for different combinations. The thickness of various combination is reported in Table 14.

Figure 15 shows perpetual pavement sections designed. It can be seen that the use of SBS modified binder with and without addition of TPO reduces layer thickness

as compared to VG 30. Pavement combination of BL+GSB layers has least overall thickness but has the largest thickness of bituminous layer whereas combination of BL+AIL+CTB+GSB has least thickness of bituminous layer. Combination of BL+WMM+GSB layers will have the largest overall thickness but less bituminous layer thickness than BL+GSB composition. Bituminous layer thickness in case of S3 and S3/T1 is reduced in every type of combination compared to VG 30. The trend as per the binder considered in decreasing order of overall thickness of pavement is VG 40<S3<S3/T1<VG 30, which remains consistent through all the four types of combinations discussed here.

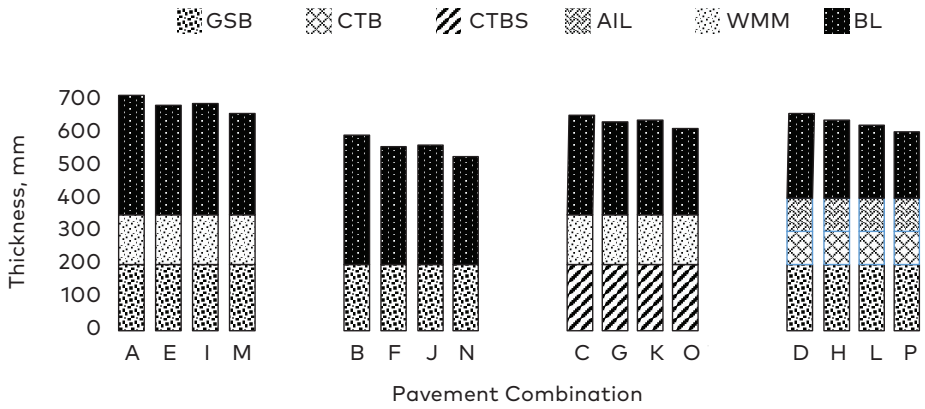

Figure 15. Pavement thickness of trial combinations

5.1. Life cycle cost calculation

To evaluate the feasibility and cost-effectiveness of different pavement designs, this study conducted a Life Cycle Cost Analysis (LCCA) spanning 50 years, focusing on a one-kilometre length of perpetual pavements with a width of 14 m. The analysis utilised the Net Present Value (NPV) method, with a 10% discount rate to convert future costs into present value and a 5% inflation rate (Cement Manufacturers' Association, 2006). Following MoRTH guidelines, which suggest a 25 mm Bituminous Course (BC) layer overlay every 5 years for routine maintenance, the study considered factors such as initial construction cost, periodic maintenance expenses like overlays, and the life cycle cost over five decades. The calculation of periodic maintenance costs accounted for inflation in prices over half of the design period. This approach was based on insights from academia, road construction engineers, and relevant literature. The life cycle cost comparison was conducted for a 14-meter width road spanning 1000 m, using the schedule of rates over three

years in Maharashtra. Labour rates, outlined in Table 15, were integrated into the analysis. This comprehensive assessment spanned three years, analysing the impact of inflation to ascertain the economic viability of perpetual pavements in India. A sample calculation for the year 2021 is presented in Table 16, while Table 17 provides a breakdown of life-cycle cost analysis per KM and maintenance costs from 2021 to 2023.

The overall life cycle cost calculation is presented in Table 17. Using modified VG 30 bitumen binder in the pavement results in a thickness of 4% to 6% greater than VG 40. According to the 2022 schedule of rates for the Maharashtra state government, VG 40 is approximately 6% more expensive than VG 30. Thus, adopting modified VG 30, as recommended in this study, could serve as a viable alternative, offsetting some of the increased cost incurred due to reduced thickness compared to unmodified binder. Table 17 indicates that the pavement combinations, in descending order of overall cost, are BL+AIL+CTB+GSB, BL+CTSB+GSB, BL+GSB, and BL+WMM+GSB. It is evident that any increase in bitumen cost will likely alter this order in the future.

Table 15. Schedule of rates for the year 2021, 2022, 2023 in the state of Maharashtra

(As per 1US $= 74.30 INR)

Material	Rate, US $/m^3			MoRT&H specification clause number
	2023	2022	2021	
CTSB	30.76	28.66	25.60	404
WMM	26.45	24.03	22.30	406
GSB/AIL	25.54	23.83	21.50	401
BC (VG 30)	106.95	90.63	92.35	507
DBM (VG 30)	99.28	84.91	87.25	505
BC (VG 40)	112.50	95.90	95.44	507
DBM (VG 40)	104.44	89.85	87.07	505
CTB	28.80	27.73	24.58	404

Table 16. Year-wise maintenance cost for perpetual pavement as per schedule of rates of year 2021

Year	Maintenance Activity	Cost per km for a 14 m wide road, thousands of US $	Inflation per annum, thousands of US $	NPV, thousands of US $
5th	Overlay of 25 mm	32.32	41.25	25.61
10th		32.32	52.65	20.30
15th		32.32	67.20	16.09
20th		32.32	85.76	12.75
25th		32.32	109.46	10.10
30th		32.32	139.70	8.01
35th		32.32	178.29	6.34
40th		32.32	227.55	5.03
45th		32.32	290.42	3.98
50th	Reconstruction work in 50th year as per concept of perpetual pavement			
			Total	108.21

Table 17. Life-cycle cost analysis per KM for proposed conventional pavement and four combinations of perpetual pavement with respect to NPV for period of 50 years

Pavement type	Year of schedule of rates	Initial construction, thousands of US $	Net present value, thousands of US $, per km			% Extra cost compared to VG 40 as binder in corresponding year
			Maintenance	Major maintenance/ Reconstruction during service period	Total	
A	2023	632.80	197.78	125.32	955.90	7.26
	2022	549.14	171.63	106.19	826.96	6.66
	2021	550.34	172.01	108.21	830.56	11.04
E	2023	591.10	184.75	125.32	901.17	1.12
	2022	513.48	160.49	106.19	780.15	0.62
	2021	513.70	160.55	108.21	782.46	4.61
I	2023	598.05	186.92	125.32	910.29	2.14
	2022	519.42	162.34	106.19	787.95	1.63
	2021	519.80	162.46	108.21	790.48	5.68
M	2023	578.69	180.87	131.62	891.18	-
	2022	505.08	157.86	112.37	775.31	-
	2021	484.68	151.48	111.83	747.99	-

	2023	618.95	193.45	125.32	937.72	9.46
B	2022	534.34	167.01	106.19	807.53	8.82
	2021	540.16	168.82	108.21	817.19	13.73
	2023	570.30	178.25	125.32	873.87	2.01
F	2022	492.73	154.00	106.19	752.92	1.46
	2021	497.40	155.46	108.21	761.07	5.92
	2023	577.25	180.42	125.32	882.99	3.07
J	2022	498.67	155.86	106.19	760.72	2.51
	2021	503.51	157.37	108.21	769.09	7.04
	2023	552.39	172.65	131.62	856.66	-
N	2022	479.78	149.95	112.37	742.10	-
	2021	462.23	144.47	111.83	718.53	-
	2023	564.02	176.28	125.32	865.62	5.05
C	2022	491.34	153.57	106.19	751.09	4.50
	2021	488.53	152.69	108.21	749.43	8.45
	2023	536.22	167.59	125.32	829.13	0.62
G	2022	467.56	146.14	106.19	719.89	0.16
	2021	464.10	145.05	108.21	717.36	3.81
	2023	543.17	169.77	125.32	838.26	1.73
K	2022	473.51	147.99	106.19	727.69	1.24
	2021	470.21	146.96	108.21	725.38	4.97
	2023	527.51	164.87	131.62	824.00	-
O	2022	462.00	144.40	112.37	718.77	-
	2021	441.30	137.93	111.83	691.06	-
	2023	432.52	135.18	125.32	693.02	13.01
D	2022	382.60	119.58	106.19	608.37	12.17
	2021	375.12	117.24	108.21	600.57	16.50
	2023	404.72	126.50	125.32	656.54	7.06
H	2022	358.82	112.15	106.19	577.16	6.42
	2021	350.69	109.61	108.21	568.51	10.28
	2023	383.87	119.98	125.32	629.17	2.60
L	2022	340.99	106.58	106.19	553.76	2.10
	2021	332.37	103.88	108.21	544.46	5.61
	2023	366.93	114.68	131.62	613.24	-
P	2022	327.59	102.39	112.37	542.35	-
	2021	307.56	96.13	111.83	515.52	-

5.2. Carbon dioxide gas emission

The calculations for embodied CO_2 were based on data sourced from the carbon and energy inventory (Hammond & Jones, 2008) and the Auroville Earth Institute study (Maini & Thautam, 2009), as elaborated in Table 18. Table 19 provides a generalized breakdown of material proportions across different pavement layers, citing MoRT&H specifications, IRC SP:49 (2014), IRC SP:53 (2010), and IRC SP:89 (2010). The embodied CO_2 values for the various pavement layers are summarised in Table 20.

Table 18. Embodied CO_2, kg/kg material

Material	Embodied CO_2
Coarse aggregate	0.0216
Cement	0.83
Fine aggregate	0.002
Bitumen	0.48
SBS	0.18

The methodology for calculating the embodied CO_2 for each pavement layer involves the following formula: Embodied CO_2 for 1 m^3 of pavement layer (kg) = 1 m^3 × Density × ((fine aggregates by mass % × embodied CO_2 of fine aggregates) + (coarse aggregates by mass (%) × embodied CO_2 of coarse aggregate) + (bitumen by mass (%) × embodied CO_2 of bitumen)).

For instance, to calculate the Embodied CO_2 for a 1 m^3 layer of BC, the following calculation is performed:

1 × 2400 × ((0.945 × 0.45 × 0.002) + (0.945 × 0.55 × 0.0216) + (0.055×0.48)) = 92.34 kg.

Similar calculations for the remaining layers are detailed in Table 19. Additional calculations were conducted considering OBC values of 5.2, 5.4, and 5.6, as discussed in Section 4.5, with the incorporation of TPO and SBS, as depicted in Table 20. Similarly, calculations for remaining layers have been reported in Table 19. Calculations considering OBC of 5.2, 5.4 and 5.6 as mentioned in Section 4.5 were also carried out with consideration of addition of TPO and SBS as shown in Table 20.

Table 19. Generalised properties of pavement layers as per MoRTH (2013) guidelines

Properties	Pavement layers					
	AIL	WMM	CTSB	DBM	GSB	BC
Cement by mass, %		-	2	-	-	-
Aggregates by mass, %	100	100	98	95.5	100	94.5
Bitumen by mass, %		-	-	4.5	-	5.5
Density, kg/m^3	2300	2300	2300	2300	2300	2400
Coarse fraction of total aggregates, %	70	70	80	60	80	55
Fine fraction of total aggregates, %	30	30	20	40	20	45
Embodied CO_2 for 1/m^3	36.15	36.15	78.03	79.90	40.66	92.34

Table 20. Embodied CO_2 for various binders

Binder Details	VG 30	S3	S3/T1	VG 40
OBC (percentage by wt. of mix)	5.2	5.6	5.4	5.4
Embodied CO_2 for 1/m^3	87.41	86.86	88.032	91.7
SBS	-	5.4	5.4	-
TPO	-	-	1.18	-
Embodied CO_2 for 1/m^3	87.41	92.26	94.61	91.7

Initial carbon dioxide emission for construction as well as overall emission considering five decades of service for different pavement sections with OBC discussed in the study is worked out in Table 21. Embodied CO_2 for TPO is considered around 0.13 kg per kg of material (Banar, 2015). Table 21 shows that as an alternative to VG 30 grade binder, modified VG 30 binder with and without TPO, can help reduce CO_2 emission significantly. If comparison of modified binder with unmodified VG 40 binder is done, the difference in CO_2 emission is small. Hence, in absence of availability of VG 40 binder, modified VG 30 binder can also be advocated for perpetual pavements in context of environmental aspect.

Table 21. Total CO_2 emission for proposed pavement combinations

Pavement type and binder	CO_2 emission, tons			% Increase in CO_2 emission compared to VG 40 binder in bituminous layer
	Initial construction	Maintenance activity/ reconstruction activity	Total	
A (VG 30)	633.5	924.371	1557.871	7.11
E (S3)	616.0602	906.9312	1522.991	4.72
I (S3/T1)	631.8949	922.7659	1554.661	6.89
M (VG 40)	581.77	872.641	1454.411	-
B (VG 30)	594.272	885.143	1479.415	9.27
F (S3)	572.4362	863.3072	1435.743	6.04
J (S3/T1)	589.0934	879.9644	1469.058	8.50
N (VG 40)	531.531	822.402	1353.933	-
C (VG 30)	664.762	955.633	1620.395	4.67
G (S3)	656.1142	946.9852	1603.099	3.55
K (S3/T1)	670.3039	961.1749	1631.479	5.38
O (VG 40)	628.635	919.506	1548.141	-
D (VG 30)	730.3205	1021.192	1751.512	7.11
H (S3)	718.5794	1009.45	1728.03	5.67
L (S3/T1)	704.7978	995.6688	1700.467	3.99
P (VG 40)	672.196	963.067	1635.263	-

Conclusion

This study investigated the performance of SBS-modified VG 30 grade bitumen, both with and without TPO addition, through a number of tests encompassing penetration, ductility, elastic recovery, softening point, viscosity, rheological properties, and morphological observations. Optimal SBS content for VG 30 base bitumen modification and the ideal TPO content for SBS-modified VG 30 binder were determined. Marshall stability and ITS tests were conducted on modified bitumen with the optimal additive content alongside base bitumen. Sixteen perpetual pavement sections were designed and compared, each featuring four combinations for VG 30, VG 40, S3, and S3/T1. The following conclusions were drawn:

Increased SBS dosage led to higher softening point and viscosity, with TPO addition further increasing consistency and temperature sensitivity. Although SBS addition decreased penetration value, TPO addition counteracted this effect, enhancing binder consistency. Additionally, increased SBS content improved ductility and elastic recovery, indicating enhanced low-temperature performance.

Modification of VG 30 bitumen with SBS, followed by TPO, elevated the high-temperature PG grading from PG 64 to PG 70, with TPO addition proving most beneficial. Modified binders generally outperformed base binders across laboratory tests. Binder performance rankings for rut resistance varied slightly at 60 °C but generally aligned with G^*, $G^*/\sin\delta$[9], and Shenoy parameter results, with binder S3 exhibiting superior rut resistance.

TPO addition in SBS-modified binder reduced mixing and compaction temperature, with the HSR method indicating lower values compared to the equiviscous method. This temperature reduction was attributed to the lower viscosity associated with TPO presence, suggesting a non-Newtonian behaviour for modified bitumen.

SBS-modified bitumen necessitated a higher OBC due to its elevated viscosity compared to VG 30, while TPO addition reduced OBC by lowering binder viscosity. Marshall stability values for SBS-modified binders, with or without TPO, surpassed those of VG 30, highlighting the stability benefits of stiffer binders.

SBS-modified bitumen, with or without TPO, exhibited higher ITS values than VG 30 but lower than VG 40, indicating suitability for perpetual pavement applications.

SBS-modified VG 30, with or without TPO, emerges as a viable alternative to VG 40, offering cost and carbon dioxide emission reductions while addressing VG 40 availability issues in India. Additionally, the composite modification of bitumen with SBS and TPO provides a sustainable solution and repurposes waste tires.

Overall, the results advocate for SBS and TPO use as modifiers to enhance rutting resistance in bituminous binders, potentially benefiting perpetual pavement design. Further research could delve into elucidating the mechanisms behind this relationship and optimising SBS and TPO proportions. Long-term field evaluations are also warranted to validate their efficacy in mitigating rutting in practical pavement applications.

Data availability

The dataset generated, analysed, and/or used during the current study is available from the corresponding author upon reasonable request.

Declarations

The authors have no competing interests to declare.

REFERENCES

AASHTO TP 5. (1994). *Dynamic shear rheometer standard test method for asphalt binder rheological properties determination*. American Association of State Highway and Transportation Officials.

Airey, G. D. (2003). Rheological properties of styrene butadiene styrene polymer modified road bitumens. *Fuel*, *82*(14), 1709–1719. https://doi.org/10.1016/S0016-2361(03)00146-7

Anderson, D. A., Christensen, D. W., Bahia, H. U., Dongre, R., Sharma, M. G., Antle, C. E., & Button, J. (1994). *Binder characterization and evaluation-physical characterization*. Strategic Highway Research Program (SHRP-A-369), National Research Council, Washington, DC.

Ansari, A. H., Jakarni, F. M., Muniandy, R., Hassim, S., & Elahi, Z. (2021). Natural rubber as a renewable and sustainable bio-modifier for pavement applications: A review. *Journal of Cleaner Production*, *289*, Article 125727. https://doi.org/10.1016/j.jclepro.2020.125727

ASTM D 2493. (2010). *Standard viscosity-temperature chart for asphalts*. ASTM International, West Conshohocken, PA.

ASTM D 4402. (2012). *Standard test method for viscosity determination of asphalt at elevated temperatures using a rotational viscometer*. ASTM International, West Conshohocken, PA.

ASTM D 6927. (2016). *Standard test method for Marshall stability and flow of asphalt mixtures*. ASTM International, West Conshohocken, PA.

ASTM D 6931. (2017). *Standard test method for indirect tensile (IDT) strength of asphalt mixtures*. ASTM International, West Conshohocken, PA.

ASTM D 7405. (2015). *Standard test method for multiple stress creep and recovery of asphalt binder using a dynamic shear rheometer*. ASTM International, West Conshohocken, PA.

ASTM-D 6373. (1999). *Performance graded asphalt binder standard specification*. American Society for Testing and Materials.

Banar, M. (2015). Life cycle assessment of waste tire pyrolysis. *Fresenius Environmental Bulletin*, *24*(4), 1215–1226. https://www.researchgate.net/publication/282173325_Life_cycle_assessment_of_waste_tire_pyrolysis

Bouldin, M. G., Dongré, R., & D'Angelo, J. (2001). Proposed refinement of superpave high-temperature specification parameter for performance-graded binders. *Transportation Research Record: Journal of the Transportation Research Board*, *1766*(1), 40–47. https://doi.org/10.3141/1766-06

Cement Manufacturers' Association. (2006). Cement concrete roads v/s bituminous roads – A cost analysis. *Grameen Sampark*, 28–31. https://kabirinfra.wordpress.com/wp-content/uploads/2014/10/pmgsy-kabirinfra.pdf

Chaala, A., Ciochina, O. G., & Roy, C. (1999). Vacuum pyrolysis of automobile shredder residues: use of the pyrolytic oil as a modifier for road bitumen. *Resources, Conservation and Recycling*, *26*(3–4), 155–172. https://doi.org/10.1016/s0921-3449(99)00003-8

Chen, A., Deng, Q., Li, Y., Bai, T., Chen, Z., Li, J., Feng, J., Wu, F., Wu, S., Liu, Q., & Li, C. (2022). Harmless treatment and environmentally friendly application of waste tires – TPCB/TPO composite-modified bitumen. *Construction and Building Materials*, *325*, Article 126785. https://doi.org/10.1016/j.conbuildmat.2022.126785

Cortizo, M. S., Larsen, D. O., Bianchetto, H., & Alessandrini, J. L. (2004). Effect of the thermal degradation of SBS copolymers during the ageing of modified asphalts. *Polymer Degradation and Stability*, *86*(2), 275–282. https://doi.org/10.1016/j.polymdegradstab.2004.05.006

D'Angelo, J. A. (2009). The relationship of the MSCR test to rutting. *Road Materials and Pavement Design*, *10*(sup1), 61–80. https://doi.org/10.1080/14680629.2009.9690236

D'Angelo, J., Kluttz, R., Dongre, R. N., Stephens, K., & Zanzotto, L. (2007). Revision of the Superpave high-temperature binder specification: multiple stress creep recovery test. *Journal of the Association of Asphalt Paving Technologists*, *76*, 47–79.

Dongré, R., D'Angelo, J., Reinke, G., & Shenoy, A. (2004). New criterion for Superpave high-temperature binder specification. *Transportation Research Record*, *1875*(1), 22–32. https://doi.org/10.3141/1875-04

Elkashef, M., Podolsky, J., Williams, R. C., & Cochran, E. W. (2017). Introducing a soybean oil-derived material as a potential rejuvenator of asphalt through rheology, mix characterisation and Fourier transform infrared analysis. *Road Materials and Pavement Design*, *19*(8), 1750–1770. https://doi.org/10.1080/14680629.2017.1345781

Emery, S. J., & O'Connell, J. (1999). High-performance SBS modified binder development. *Proceedings of the 7th Conference on Asphalt Pavements for Southern Africa*, *CAPSA*.

Fini, E. H., Kalberer, E. W., Shahbazi, A., Basti, M., You, Z., Ozer, H., & Aurangzeb, Q. (2011). Chemical characterization of biobinder from swine manure: Sustainable modifier for aAsphalt binder. *Journal of Materials in Civil Engineering*, *23*(11), 1506–1513. https://doi.org/10.1061/(asce)mt.1943-5533.0000237

Formela, K. (2021). Sustainable development of waste tires recycling technologies – recent advances, challenges and future trends. *Advanced Industrial and Engineering Polymer Research*, *4*(3), 209–222. https://doi.org/10.1016/j.aiepr.2021.06.004

Hammond, G., & Jones, C. (2008). *Inventory of carbon & energy: ICE*. Department of Mechanical Engineering, University of Bath, UK. https://perigordvacance.typepad.com/files/inventory-ofcarbonandenergy.pdf

Hugener, M., Partl, M. N., & Morant, M. (2013). Cold asphalt recycling with 100% reclaimed asphalt pavement and vegetable oil-based rejuvenators. *Road Materials and Pavement Design*, *15*(2), 239–258. https://doi.org/10.1080/14680629.2013.860910

IRC 37. (2012 and 2018). *Tentative guidelines for flexible pavement design*. Indian Road Congress, New Delhi, India.

IRC SP:49. (2014). *Guidelines for the use of dry lean concrete as sub-base for rigid pavement* (first revision). Indian Road Congress.

IRC SP:53. (2010). *Guidelines on use of modified bitumen in road construction* (second revision) Indian Road Congress.

IRC SP:89. (2010). *Guidelines for soil and granular material stabilization using cement lime and fly ash*. Indian Road Congress.

Kennedy, T. W., Huber, G. A., Harrigan, E. T., Cominsky, R. J., Hughes, C. S., Von Quintus, H., & Moulthrop, J. S. (1994). *Superior performing asphalt pavements (Superpave): The product of SHRP asphalt research program*. https://www.trb.org/publications/shrp/SHRP-A-410.pdf

Lastra-González, P., Lizasoain-Arteaga, E., Castro-Fresno, D., & Flintsch, G. (2022). Analysis of replacing virgin bitumen by plastic waste in asphalt concrete mixtures. *International Journal of Pavement Engineering*, *23*(8), 2621–2630. https://doi.org/10.1080/10298436.2021.1884863

Lehmann, C. M. B., Rostam-Abadi, M., Rood, M. J., & Sun, J. (1998). Reprocessing and reuse of waste tire rubber to solve air-quality related problems. *Energy & Fuels*, *12*(6), 1095–1099. https://doi.org/10.1021/ef9801120

Lv, S., Liu, J., Peng, X., & Jiang, M. (2021). Laboratory experiments of various bio-asphalt on rheological and microscopic properties. *Journal of Cleaner Production*, *320*, Article 128770. https://doi.org/10.1016/j.jclepro.2021.128770

Lyu, L., Li, D., Chen, Y., Tian, Y., & Pei, J. (2021). Dynamic chemistry based self-healing of asphalt modified by diselenide-crosslinked polyurethane elastomer. *Construction and Building Materials*, *293*, Article 123480. https://doi.org/10.1016/j.conbuildmat.2021.123480

Maini, S., & Thautam, V. (2009). *Embodied energy of various materials and technologies*. Auroville Earth Institute (AEI), Tamil Nadu, India.

Masson, J.-F., Collins, P., Robertson, G., Woods, J. R., & Margeson, J. (2003). Thermodynamics, phase diagrams, and stability of bitumen-polymer blends. *Energy & Fuels*, *17*(3), 714–724. https://doi.org/10.1021/ef0202687

Mastral, A. M., Callén, M. S., Murillo, R., & GarcÍa, T. (1999). Combustion of high calorific value waste material: Organic atmospheric pollution. *Environmental Science & Technology*, *33*(23), 4155–4158. https://doi.org/10.1021/es990289o

Mittal, A., Arora, K., Kumar, G., & Jain, P. K. (2018). Comparative studies on performance of bituminous mixes containing laboratory developed hard grade bitumen. *Advances in Civil Engineering Materials*, *7*(2), 92–104. https://doi.org/10.1520/acem20170039

Morea, F., Agnusdei, J. O., & Zerbino, R. (2011). The use of asphalt low shear viscosity to predict permanent deformation performance of asphalt concrete. *Materials and Structures*, *44*, 1241–1248. https://doi.org/10.1617/s11527-010-9696-3

Movilla-Quesada, D., Raposeiras, A. C., Silva-Klein, L. T., Lastra-González, P., & Castro-Fresno, D. (2019). Use of plastic scrap in asphalt mixtures added by dry method as a partial substitute for bitumen. *Waste Management*, *87*, 751–760. https://doi.org/10.1016/j.wasman.2019.03.018

Murugan, S., Ramaswamy, M. C., & Nagarajan, G. (2009). Assessment of pyrolysis oil as an energy source for diesel engines. *Fuel Processing Technology*, *90*(1), 67–74. https://doi.org/10.1016/j.fuproc.2008.07.017

Narayan, S. P. A., Little, D. N., & Rajagopal, K. R. (2019). Incorporating disparity in temperature sensitivity of asphalt binders into high-temperature specifications. *Journal of Materials in Civil Engineering*, *31*(1). https://doi.org/10.1061/(asce)mt.1943-5533.0002534

NCHRP. (2004). *Guide for mechanistic-empirical design of new and rehabilitated pavement structures* (Project 1-37A). National Cooperative Highway Research Program (NCHRP), Washington, DC.

Niu, D., Xie, X., Zhang, Z., Niu, Y., & Yang, Z. (2021). Influence of binary waste mixtures on road performance of asphalt and asphalt mixture. *Journal of Cleaner Production*, *298*, Article 126842. https://doi.org/10.1016/j.jclepro.2021.126842

Ranadive, M. S., Hadole, H. P., & Padamwar, S. V. (2018). Stone matrix asphalt and asphalt concrete performance using modifiers. *ASCE Journal of Civil Engineering*, *22*(1), 361–374. https://doi.org/10.1061/(ASCE)MT.1943-5533.0002107

Rowhani, A., & Rainey, T. (2016). Scrap tyre management pathways and their use as a fuel – A review. *Energies*, *9*(11), Article 888. https://doi.org/10.3390/en9110888

Roy, C., Chaala, A., & Darmstadt, H. (1999). The vacuum pyrolysis of used tires: End-uses for oil and carbon black products. *Journal of Analytical and Applied Pyrolysis*, *51*(1–2), 201–221. https://doi.org/10.1016/S0165-2370(99)00017-0

Saboo, N., & Kumar, P. (2016). Analysis of different test methods for quantifying rutting susceptibility of asphalt binders. *Journal of Materials in Civil Engineering*, *28*(7). https://doi.org/10.1061/(asce)mt.1943-5533.0001553

Shenoy, A. (2001). High temperature performance grade specification of asphalt binder from the material's volumetric-flow rate. *Materials and Structures*, *34*(10), 629–635. https://doi.org/10.1007/bf02482130

Shenoy, A. (2008). Nonrecovered compliance from dynamic oscillatory test vis-à-vis nonrecovered compliance from multiple stress creep recovery test in the dynamic shear rheometer. *International Journal of Pavement Engineering*, *9*(5), 329–341. https://doi.org/10.1080/10298430701635095

Sybilski, D. (1996). Zero-shear viscosity of bituminous binder and its relation to bituminous mixture's rutting resistance. *Transportation Research Record: Journal of the Transportation Research Board*, *1535*(1), 15–21. https://doi.org/10.1177/0361198196153500103

Tabatabaee, H. A., & Kurth, T. L. (2017). Analytical investigation of the impact of a novel bio-based recycling agent on the colloidal stability of aged bitumen. *Road Materials and Pavement Design*, *18*(sup2), 131–140. https://doi.org/10.1080/14680629.2017.1304257

Tayfur, S., Ozen, H., & Aksoy, A. (2007). Rutting performance investigation of asphalt mixtures containing polymer modifiers. *Construction and Building Materials*, *21*(2), 328–337. https://doi.org/10.1016/j.conbuildmat.2005.08.014

White, G. (2017). Grading highly modified binders by multiple stress creep recovery. *Road Materials and Pavement Design*, *18*(6), 1322–1337. https://doi.org/10.1080/14680629.2016.1212730

Xiao, F., Amirkhanian, S., Putman, B., & Shen, J. (2010). Laboratory investigation of engineering properties of rubberized asphalt mixtures containing reclaimed asphalt pavement. *Canadian Journal of Civil Engineering*, *37*(11), 1414–1422. https://doi.org/10.1139/l10-070

Xu, X., Leng, Z., Lan, J., Wang, W., Yu, J., Bai, Y., Sreeram, A., & Hu, J. (2021). Sustainable practice in pavement engineering through value-added collective recycling of waste plastic and waste tyre rubber. *Engineering*, *7*(6), 857–867. https://doi.org/10.1016/j.eng.2020.08.020

Yildirim, Y., Solaimanian, M., & Kennedy, T. W. (2000). *Mixing and compaction temperatures for hot mix asphalt concrete* (Report No. 1250-5). University of Texas at Austin. Center for Transportation Research. https://library.ctr.utexas.edu/ctr-publications/1250-5.pdf

Yousefi, A. A. (2004). Rubber-polyethylene modified bitumens. *Iranian Polymer Journal*, *13*(2), 101–112. https://www.researchgate.net/publication/238066498_Rubber-polyethylene_Modified_Bitumens

Yu, Q. X. (2008). Recycling conditions and development trend of waste tires all over the world. *China Tire Resources Recycl*., *10*, 26–36.

Zhang, B., Chen, H., Zhang, H., Kuang, D., Wu, J., & Zhang, X. (2019). A study on physical and rheological properties of rubberized bitumen modified by different methods. *Materials*, *12*(21), Article 3538. https://doi.org/10.3390/ma12213538

Zhang, Q., Wang, T., Fan, W., Ying, Y., & Wu, Y. (2014). Evaluation of the properties of bitumen modified by SBS copolymers with different styrene-butadiene structure. *Journal of Applied Polymer Science*, *131*(12). https://doi.org/10.1002/app.40398